Parametric Comparison of Floatover Barge Motions for Regular Waves

by

Tan Seok Yee

Dissertation submitted in partial fulfilment of
the requirements for the
Bachelor of Engineering (Hons)
(Civil Engineering)

DEC 2011

Universiti Teknologi PETRONAS
Bandar Seri Iskandar
31750 Tronoh
Perak Darul Ridzuan

CERTIFICATION OF APPROVAL

Parametric Comparison of Floatover Barge Motions for Regular Waves

by

Tan Seok Yee

A project dissertation submitted to the
Civil Engineering Programme
Universiti Teknologi PETRONAS
in partial fulfilment of the requirement for the
BACHELOR OF ENGINEERING (Hons)
(CIVIL ENGINEERING)

Approved by,

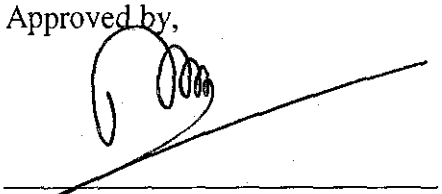

(Professor Dr. Kurian V. John)

Project Supervisor

Universiti Teknologi PETRONAS

Tronoh, Perak

Dec 2011

CERTIFICATION OF ORIGINALITY

This is to certify that I am responsible for the work submitted in this project, that the original work is my own except as specified in the references and acknowledgements, and that the original work contained herein have not been undertaken or done by unspecified sources or persons.

_____

TAN SEOK YEE

ABSTRACT

Following advancements in the offshore technology, facilities required have resulted in heavier topside loading for recent platform designs. However, the lift crane vessels conventionally used for deck (topside) installation is not up to par. In other words, conventional installations are no longer capable of catering to the offshore industry requirements. Thus, giving rise to the need for floatover installation that provides significant advantages over other methods of deck installation for heavy topsides, especially in areas of the world where access to heavy construction equipment, trained labour and supplies are not readily available or reliable.

Due to the relatively foreign technology of floatover installation, research efforts are being made to understand the motion responses of a floatover barge during its entire operation from standby to mating of topside and support legs to exit. Therefore, this project is a collaboration between Technip Geoproduction (M) Sdn Bhd and Universiti Teknologi Petronas (UTP) to conduct research on the float-over installation used for a fixed jacket structure, Owez ODP-A in the Caspian Seas. The research will be done mainly using model tests and numerical analysis.

From model tests and numerical analysis, resulting RAO of the barge model along with the corresponding motion response will be analyzed to fully understand the loads triggered by environmental loadings and the resulting barge motions. With that understanding, the series of ballasting load for transfer of topside onto jacket legs can be determined to ensure minimum barge impact toward the fender system at the substructure. This knowledge can then be utilized to mature floatover installation for jacket structures in Malaysian seas, an unprecedented method for our region.

ACKNOWLEDGEMENT

I have taken efforts in this project. However, none of this would have been possible without the kind support and encouragement of many individuals. Thus, I would like to take this opportunity to extend my sincere gratitude to each and every one of them.

First and foremost, I am highly indebted to my supervisor, Professor Dr. Kurian V. John for his direction, assistance as well as guidance throughout the course of my final year project. Without his supervision and constant support, my project would not have been as smooth-sailing; neither would it have been as progressive.

My utmost acknowledgement also goes out to the Masters students, Ms Husna and Ms Zaidah who are also involved in the study of floatover barge motions but at a more extensive level. A big contribution in terms of theoretical knowledge and model testing procedures from the both of them throughout the past few months has been great indeed. My project would be less of a success if not for their enthusiasm and eager helpfulness.

I would also like to thank Mr Meor and Mr Idris, the offshore lab technicians that have gone through countless hours of overtime just to assist us in completing the model tests. Not forgetting, my fellow course mate, Shawn who have willingly helped me out with his abilities for his kind co-operation.

Last but not least, a great deal of appreciation is expressed towards friends, family and most importantly, God Almighty for the spiritual reinforcement and moral support.

TABLE OF CONTENTS

LIST OF FIGURES

LIST OF TABLES

CHAPTER 1
INTRODUCTION

1.1 Background Study

Deck (topside) installation has always been one of the most challenging and critical element of an offshore platform project. Conventionally, small topsides have been installed as one unit using low-capacity crane vessels and jack-ups. Medium to large topsides have been either modularized to facilitate installation with small crane vessels, or built as integrated topsides and installed either by means of heavy-lift crane vessels. For relatively light topsides in the range of less than 3000 metric tons lift cranes are readily available in most offshore areas of the world.[1] However, once topside weight surpasses the 3000 metric ton mark, the number of vessels apt to handle such load reduces significantly. Due to limited availability of heavy lift vessels and the significant costs related to the mobilization of such vessels, many projects have been based on float-over installation as a commercially viable solution as compared to conventional lifting. In addition to that, the lifting cranes are sensitive to the prevailing weather conditions at the installation site, which can even reduce lifting capacity by 40-50%.[2]

Float-over is an installation method that is generating interest from many operators who are challenged with designing heavy lift crane vessels installations. The ideal range for float-over is in water depths of 10 to 200m.[3] Float-over calls for the topside to be completed on land and then placed onto a barge (float-over barge) which will tow the structure to its respective jackets. This barge is floated between jacket legs until mating points between deck and jacket are properly aligned. Once the mating points align, the transportation barge is ballasted with water, lowering the deck onto the jacket structure. Other elements also come into play in the floatover installation process, notably the LMUs (Leg Mating Units), DMUs (Deck Mating Units) and fender systems.

LMUs are placed in steel cans known as transition pieces which are installed on top of jacket legs. These units are rubber elements mainly applied to dampen forces created as topside load is transferred to the jackets. The DMUs on the other hand are more concerned with load transfer from topside to floatover barge in the fabrication yard. DSUs positioned on the deck support frame absorb the weight of topsides as they are skidded onto the barge. Meanwhile, surge and sway fenders absorb the impact of barge on the jacket as it moves forward or sideway during the mating operation.[4]

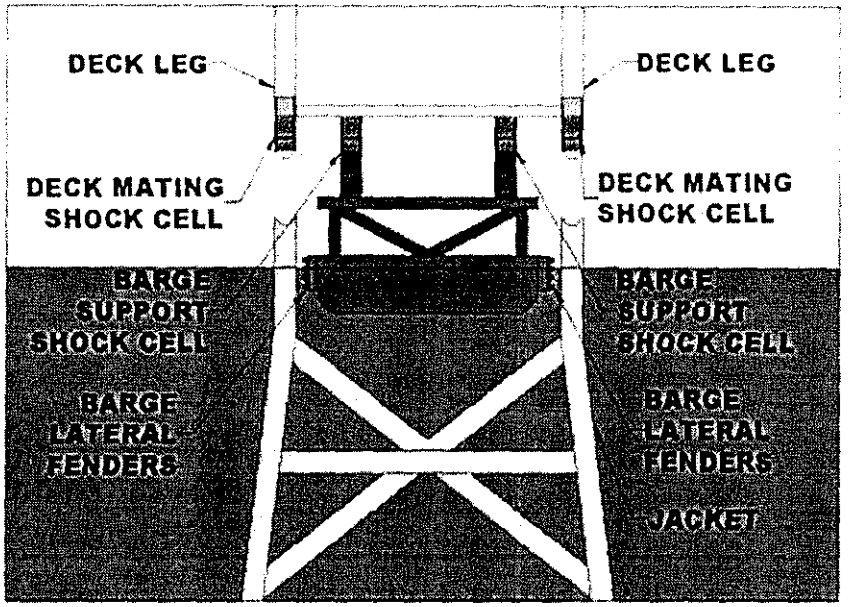

Figure 1: Elements of a floatover installation

Even with all the necessary precautions, the crucial challenge of floatover installation is still transferral of load from barge to jacket. This must be done with minimal damage to either structure, even though elements such as wave, wind and current are constantly inducing movement to barge, more often than not causing damage to fender systems at the jacket legs. Adding on to that is the complication of alignment process between deck and jacket, an already painstakingly slow procedure further impeded by environmentally induced rocking. Since very little margin of error is allowed, it is important to understand the float-over barge responses to these environmental loads during deck installation. Therefore, this project mainly aims to determine said responses using numerical analysis and experimental modelling tests.

1.2 Problem Statements

There are approximately 200 fixed jacket platforms in Malaysian waters (PMO, SBO, SKO). Thus far, installation is largely dependent on heavy lift crane vessels. Given the high demand of cranes in Malaysian offshore industry, this has contributed to the lack of crane availability for installation and hence a very narrow installation window. More often than not, topsides are not completely finished and operational on a specific date that a heavy lift vessel is scheduled for offshore installation. Operators will then be forced to tow out the unfinished deck and carry over its onshore work to the offshore location. This adds time, logistic challenges and costs to the installation work.

With that, operators in Malaysia are looking towards other methods of installations particularly float-over. The only project that utilized float-over technology in Malaysian waters was done by Technip during Kikeh spar installation (floating structure) for Murphy Oil, the first conducted outside Gulf of Mexico. Technip has also designed a float-over barge configuration that caters specifically towards deck installation for fixed jacket structures. This forked configuration is currently underway for the Owez ODP-A platform installation in Caspian seas, Turkmenistan. This project is wholly owned by Petronas Carigali (Turkmenistan) Sdn Bhd, detailed designing by Technip Geoproduction (M) Sdn Bhd.

The ballasting and de-ballasting process during alignment (mating) of the Owez-ODPA platform and its legs is very much affected by barge motions. As mentioned in the background study, even with proper fender systems also known as jacket leg protectors used to absorb vessel impact on jackets, the small gaps between float-over barge and jacket during mating process leads to a high possibility of jacket damage in the form of impact, abrasive action from vessels or even direct pressure. To reduce the barge impact on fender systems, increased ballasting loads most likely to cause damage due to barge motions are investigated in this study. Study area will be based on the ODP-A platform with the hopes to make a similar forked configured floatover barge applicable for installation of Petronas fixed offshore platforms in Malaysian seas.

Another project in Turkmenistan referred to as the MCR-A platform, a GBS structure is used as case study. Similar to ODP-A, the installation process uses floatover technology. But, the MCR-A is handpicked as case study mainly due to the fact that its floatover operation utilizes the same forked barge akin to that used for ODP-A. Model tests and numerical analysis will result in optimized theoretical formulations describing the barge's dynamic responses to environmental loadings such as random and regular waves. My studies will be focused mainly on responses due to regular waves. With theoretical formulations, dynamic responses of float-over vessels with that particular configuration when used in Malaysian seas can then be generated by substituting environmental parameters of South China Sea.

The performance of a successful float-over installation requires adequate design and analysis of each phase of the installation and a sufficient weather window in which to perform each phase.[5] The floatover method requires careful consideration of the prevalent waves and swell, not only as to height and period but also as to direction.[6] But, the atrocity here is that there is a serious lack of understanding regarding the factors affecting barge motions and until what extend these factor's effects are on barge motions.

Using float-over installation for fixed platform structures is unprecedented in Malaysian seas. Hamilton et al. (2008) stressed that the necessity for a thorough understanding of the system dynamics and environmental site data to allow the assessment of reliable loads for deck on jacket floatovers.[7] Therefore, it is important to understand the responses of a float-over vessel in Malaysian seas and the necessary considerations to be made before actual installation. By determining the responses, deck transportation and stability can be assured even before the implementation of such float-over technology in Malaysian seas.

1.3 Objectives

The main long term objective of this research work as a whole is to obtain an optimized theoretical formulation describing dynamic barge responses to environmental loadings. For my final year project, objective of my study will be established based on a support basis to the extensive work being done on a Masters level:

- To determine the dynamic responses of float-over barge subjected to regular waves with emphasis on parametric comparison
- To validate the dynamic responses by conducting model tests for the controlled reference data in the wave tank of UTP offshore laboratory.

1.4 Scope of Study

The scope of this study will be limited to unidirectional waves whereby generated waves are applied on the barge only from one certain direction. For the entire modelling of this project, barge is exposed to 6 wave directions or angles by manipulating the barge's orientation. Again, this is narrowed down towards a wave heading of 180°.

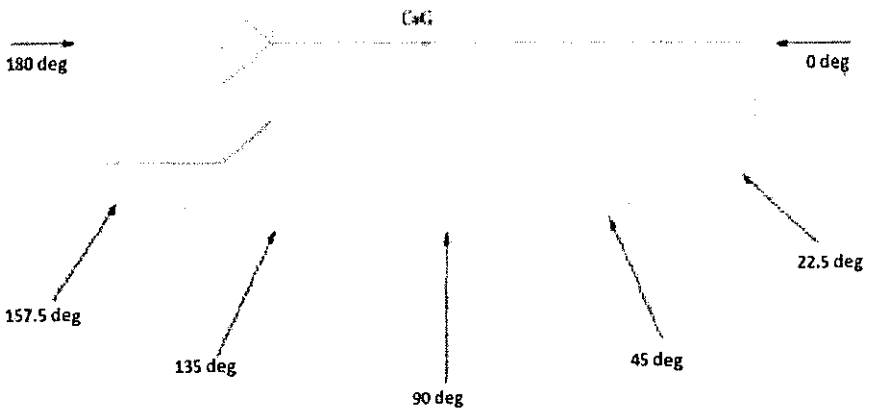

Figure 2: Wave directions simulated for model testing of floatover barge

As for vessel motions, the main directions to be considered are the surge, heave and pitch as illustrated below.

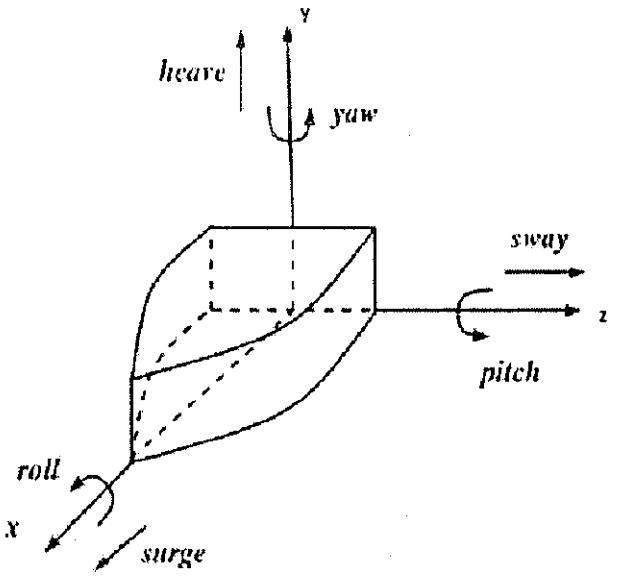

Figure 3: The 6 degrees of freedom of a floatover barge

To actualize parametric comparison for my study, I'll be focusing on a few parameters including: water depth, water draft, wave period, wave direction and mooring line stiffness. By manipulating these few parameters and then comparing it against the reference data, I can therefore determine which factor is significant to and how does it affect barge motions.

For theoretical analysis of this study, linear airy wave theory will be applied mostly to determine necessary water particle characteristics mainly acceleration and pressure. Another area of theoretical analysis is the study of wave force on the barge structure. For this aspect, Froude-Krylov theory for rectangular block will be applied.

Another limitation of this project is the model tests conducted. Due to the time constraint, experiments will only be carried out using the reference data which is based on Caspian Seas (Turkmenistan) wave conditions. Comparing theoretical results and model tests findings for reference data, the accuracy of numerical analysis can thus be justified.

CHAPTER 2
LITERATURE REVIEW

In general, a platform's installation option is ultimately dictated by its end design. However, float-over installation is experiencing a steady surge of interest from operators worldwide. From an operational point of view, there are several distinctive phase in float-over installation:[8]

1. Standby – The vessel is a safe distance from the substructure but connected to the mooring system, and last minute preparations such as preparing the vessels rapid ballast system are under way
2. Docking – Vessel makes its way between the substructure legs
3. Pre-Mating – When ballasting the vessel to match the leg mating units (LMU), it is critical that the vessel motions be limited to suit the chosen LMU geometry. In this phase, no weight transfer occurs yet.
4. Mating – Topsides is lowered onto the substructure by rapid ballasting. With that, topside weight is transferred to the jacket completely.
5. Post-Mating – A gap is created between deck support units (DSU) and vessel to ensure vessel motions will not cause contact between the two.
6. Exit – Vessel is removed from the jacket slot.

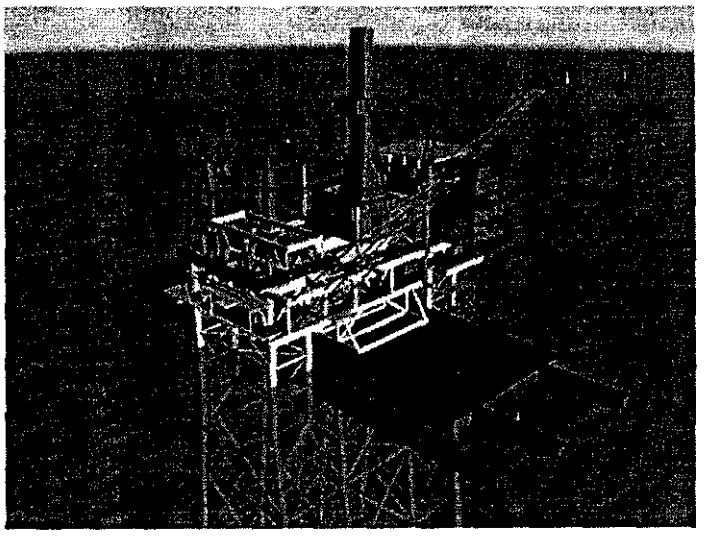

Figure 4: Barge getting into location for floatover operations

2.1 Turkmenistan Block 1[9]

The Diyarbekir and Magtymguly oil fields located in Block 1 between 30 and 100km offshore Turkmenistan, in water depths of approximately 50 to 90m is currently under development by Petronas Carigali (Turkmenistan) Sdn Bhd. The Block 1 field is an elongated field 50 to 60 km long and 10 m wide. Proposed field development plan is shown in Table 1 below. Phase 1 (1A and 1B) was given official sanction by Turkmenistan authorities in 2006. Due to subsurface uncertainties and risks, Phase 2 facilities will be subjected to possible alterations as the project progresses.

Phase	Timeframe (start-up)	Annual Average Sales Gas Production Rate (MMscfd)	Production Capacity* / Processing Facilities
1A	Start of 2009	250	Magtymguly / OGT *
1B	Middle of 2009	500	Magtymguly + Owez * / OGT*
2	End of 2015	500	Magtymguly + Owez + Diyarbekir West * / OGT
2	End of 2016	500	Magtymguly + Owez + Diyarbekir Central* / OGT

Table 1: Turkmenistan Block 1 Field Development Plan

Phase 1A, which involves production form Magtymguly includes the installation of two bridge linked platforms, namely Magtymguly Drilling Platform (MDP-A) and Magtymguly Collector Riser Platform (MCR-A). The platforms located in approximately 62m water depth were installed in 2007 and 2008 respectively. MDP-A is a nine well slot drilling platform comprising of a conventional piled substructure and minimal topsides. The installation of this platform was carried up employing the jack up rig whereas MCR-A is a steel gravity based foundation structure with float-over topsides. Due to the usage of float-over installation, MCR-A is used as a case study and will be discussed in further details in Section 2.2.

Phase 1B involves the installation and production of the Owez ODP-A facility at Owez, located in a water depth of 73.4m. The platform structure at Block 1B is a conventional jacket (fixed) platform. Like the MCR-A, the substructure is to be installed by a jack up drilling rig and the topsides by the float-over method.

2.2 MCR-A Development Project [10]

As mentioned in Chapter 1, floatover installation of the Turkmenistan MCR-A Block 1 Development Project is used as a case study. Model tests for the MCR-A was in fact conducted by DHI. Therefore, all model test procedures and wave conditions for my study will be derived from the DHI manual discussed in detail in Section 2.4. This can be rationalized in view that both platforms are part of the Block 1 Development Project. In addition to that, both platforms use the same float-over barge configuration for topside installation. Figure 5 below shows the docking process where float-over vessels are entering between the MCR-A platform's GBS legs.

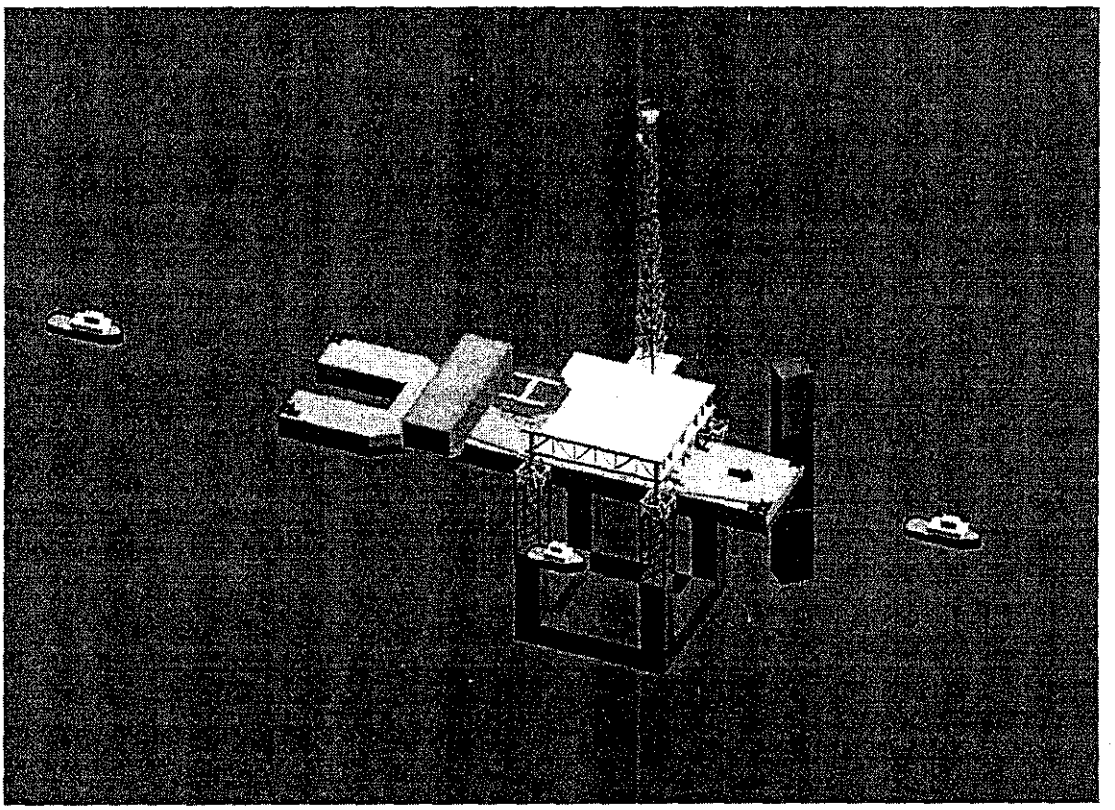

Figure 5: Topside on installation barge during barge entrance

2.2.1 Topside Description

The topside legs for MCR-A are spaced at 42m x 42m centre to centre. The deck consists of two primary levels (i.e. Upper Deck and Lower Deck) with a linked bridge to fixed platform MDP-A along with a helideck, flare boom, pedestal crane, provision for future bridge, and Building Module (comprising of Switchgear/MCC room, battery room, instrument and telecommunication room (ITR), and temporary shelter). MCR-A topside is illustrated in Figure 6.

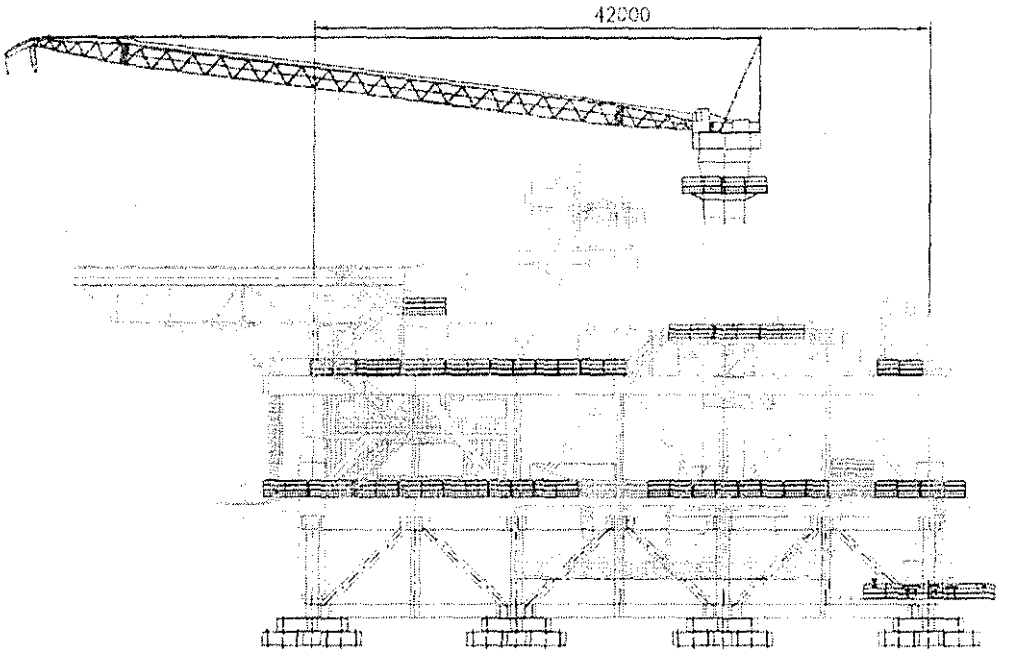

Figure 6: MCR-A topside

2.2.2 GBS Description

The geometry of the MCR-A GBS (Gravity Base Structure) consists of a square annular base with external dimensions 54 m x 54 m, with a central void 34 m x 34 m and 5 m deep skirts. The plan area of the base is 1760m^2 and the skirt walls total 472 linear metres. The underside of the base comprises twelve individual compartments, which act as separate hydraulic compartments for the purposes of installation and extraction. The skirts are to be installed to a minimum penetration depth of 4.5m. On each of the corners of the square base there are 58 m high columns. Lower part of column is of plate structure, and the top 33m of the columns comprises four 8m x 8m lattice type structures. Between the lower leg

and the topsides the structure is split into 4 bays that consist of primary vertical cross bracings. Each top bay leg contains a support chord primarily used for the topsides connection.

2.2.3 Barge description

As mentioned in the beginning of this section, the float-over barge used for deck installation of both MCR-A and ODP-A platform are of the same dimensions with length of 159.76, 30.0 m width and modified 45.72 m width fork like stern. Figure 7 below shows a side view of how the MCR-A topside is position on the barge:

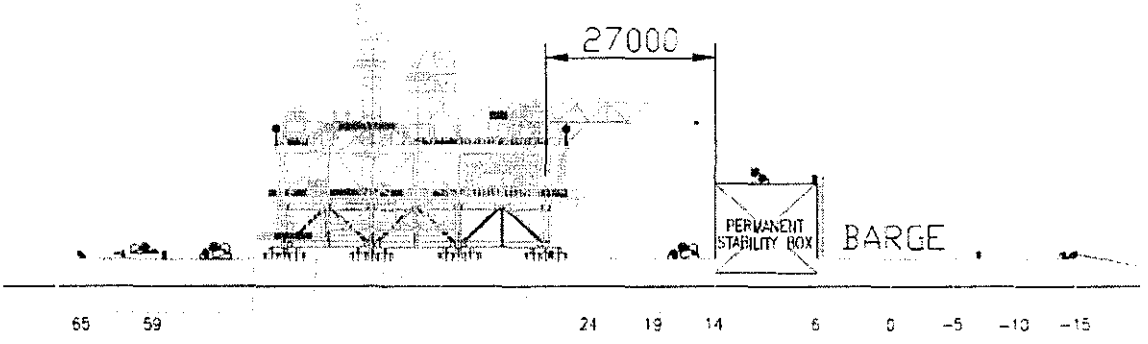

Figure 7: MCR-A topside on barge during dry tow and float-over operation

2.3 Owez ODP-A Platform [11]

PETRONAS Carigali (Turkmenistan) Sdn Bhd (PCTSB) the wholly owned exploration and production subsidiary of PETRONAS (Malaysia) is at the moment developing Turkmenistan Block 1 Gas Development Project at the Caspian Sea, Turkmenistan. The ODP-A platform currently under research by Universiti Teknologi Petronas (UTP) is located at the Owez Field in Block IB located approximately 70km south-west of Kiyanly, offshore Turkmenistan.

2.3.1 Platform Description

The Owez Drilling Platform A designed by Technip Geoproduction (M) Sdn Bhd comprises of a main platform and a Free Standing Conductor (FSC) platform. The jacket is a 4-legged fixed structure with a total of four (4) skirt piles, one (1) at each outer corner. The four (4) corner skirt legs are spaced at 23m x 30m. The

inner leg spacing is 14m x 12m. All legs are vertical – no batter. The topside legs are spaced at 14.0m in the east-west direction and 12.0m in the north-west direction, centre to centre.

2.3.2 Barge Description

The Owez ODP-A platform's topside shall be mated with the jacket substructure by a float-over method using a purpose designed and fabricated forked barge designed by Aker Offshore. The forked arrangement, at the stern of the barge, has been designed to transport the topside. Figure 8 shows a picture of the modified barge. It has two types of stability box, a permanent one situated near the stern and a removable stability box at the bow. The barge has 31 individual compartments in the hull and 6 individual compartments in each stability box, shown clearly in Figure 9. These compartments are utilized for different marine installation and transportation purposes. A brief description on the barge dimension: 159.76 m in length and 30.0 m in width with modified 45.72 m wide fork like stern. The stern lot is 15.72 m wide and 29.76 m deep. All dimensions are stated in the illustration provided of the installation barge.

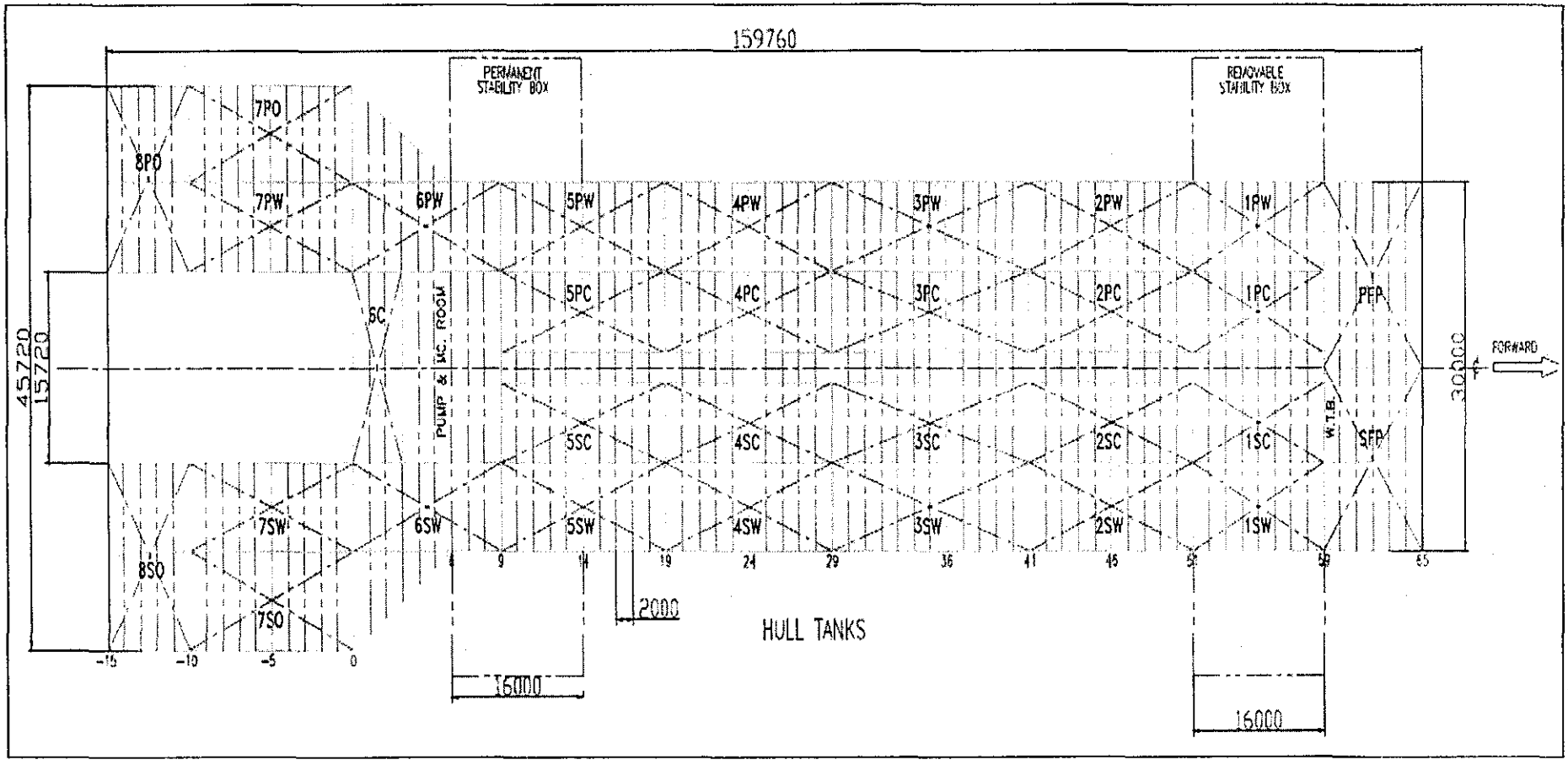

Figure 8: Plan view of floatover barge

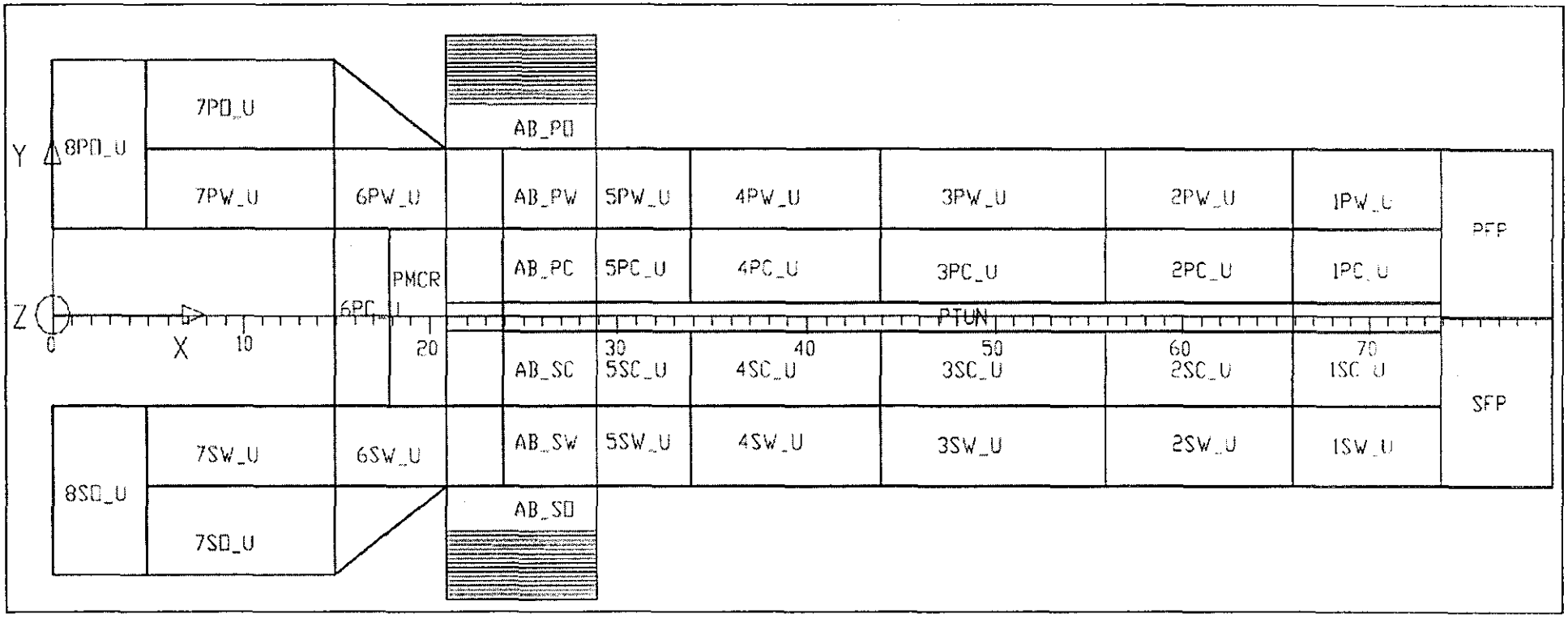

Figure 9: Compartment plan of floatover barge

2.4 MCR-A platform model tests [12]

The model test was conducted by DHI for Technip Geoproduction (M) Sdn Bhd for a coupled system consisting of an installation float-over barge and GBS (Gravity Based Structure). The GBS has to be installed at Block 1 in the Caspian Sea, Turkmenistan. The purpose of the project was to investigate the dynamic behaviour/response of the coupled system when the GBS platform is lowered towards the seabed using installation barge. The scope of work required two models: the GBS model and the installation barge, both with a scale of 1:30. The actual installation at Caspian Sea was done at a depth of 61.7m which corresponds to a model water depth of 2.06m using the same scale of 1:30. The depth of the test facility is 3.0m so in order to have the correct water depth; a platform of (4X3m) was fabricated and positioned at the testing area.

The model was used mainly to measure: the 6 degrees-of-freedom motions of the barge and GBS during all the installation and touchdown tests, forces in the 4 mooring lines on the barge and the forces in the 12 stretcher lines connecting the barge and GBS using wave conditions at three positions in the wave basin.

A total of six different sea states were specified for the model test program. They are all unidirectional and based on the JONSWAP spectrum.

Condition No	H_s (m)	T_p (s)
1	0.5	5
2	0.5	7
3	1.0	5
4	1.0	7
5	1.5	7
6	2.0	7

Table 2: Simulated wave conditions for MCR-A Platform Model Tests

2.4.1 Instruments

Several types of instruments were used to determine wave elevations and motions/loads in the coupled system. Below is a description of the different types of instruments and respective usage in the tests:

1. MarineTrak motion sensing system

   A video based motion sensing system called MarineTrak was used to monitor the motions of the model. Reflective markers were mounted on top of the GBS and on top of the barge with a dedicated PC sampling the positions of these markers. The six degrees-of-freedom rigid body motions of the barge and of the GBS were then derived from the position of the reflective markers on each of the models. All motions were determined with reference to a coordinate system defined by the centre point of the coupled system or by the model at rest at the mean mooring position. All data were logged at the designated PC during tests.

2. Wave gauges

   Wave gauges used for this project are of a conductivity type probe, which measures the change of conductivity between two steel electrodes as the water level fluctuates around the instrument. Eight of these gauges were used during calibration of the wave conditions whereas during testing, three were kept in the basin. The standard wave gauge had the following specifications:

   - Measuring range: 25cm to 100cm
   - Accuracy: Better than 0.5% F.S (Full Scale)
   - Resolution: Better than 1mm

3. Mooring line force gauges

   Two one-component tension force meters were installed at the bow corners of the barge and also at the stern corners. The gauges were used for measuring mooring line loads. The one component force gauges carried the following specifications:

   - Measuring range: ± 20kN
   - Accuracy: 1% of measured value
   - Resolution: 0.1% of force range

2.4.2 Tests set up and procedures

The tests were divided into the following test types mentioned below along with a brief description:

1. Decay tests

   The notable tests by DHI that are relevant to this project include decay tests. Decay tests determine the natural periods (for 6 degrees-of-freedom motions) and damping ratios of the barge and GBS for different load cases as depicted by the data shown below. The logarithmic decrement was found by fitting the decay response to the theoretical decay of a linearly damped (critically damped) one degree-of-freedom system.

Condition	Barge	GBS
Surge Natural Period (s)	216.4	218.5
Sway Natural Period (s)	192.9	194.8
Heavy Natural Period (s)	-	-
Roll Natural Period (s)	7.2	-
Pitch Natural Period (s)	8.0	-
Yaw Natural Period (s)	100.8	96.3
Surge Damping	0.192	0.188
Sway Damping	0.213	0.249
Heavy Damping	-	-
Roll Damping	0.058	-
Pitch Damping	0.234	-
Yaw Damping	0.117	0.150

Table 3: Decay test results from MCR-A platform model tests

2. Installation load case 1,2 and 3

   The coupled system was also tested for various load cases during the installation phase. Each test was done primarily to determine RAOs for the barge and GBS and to determine the mooring and stretcher line forces. For each load cases, a number of tests are conducted with different significant wave heights and peak periods.

- Installation Load Case 1- This load case modelled the start phase of the GBS installation.

Test No	Wave heading	H_s (m)	T_p (s)
1	Head sea (0°)	1.0	5.0
2	Head sea (0°)	1.0	7.0
3	Head sea (0°)	1.5	7.0
4	Head Oblique (22.5°)	1.0	5.0
5	Head Oblique (22.5°)	1.0	7.0
6	Beam sea (90°)	0.5	5.0
7	Beam sea (90°)	0.5	7.0

Table 4: Test conditions for DHI model tests load case 1

- Installation Load Case 2- This load case modelled the installation phase where GBS was close to the seabed without being in contact.

Test No	Wave heading	H_s (m)	T_p (s)
8	Head sea (0°)	1.0	5.0
9	Head sea (0°)	1.0	7.0
10	Head sea (0°)	1.5	7.0
11	Head quartering (45°)	1.0	5.0
12	Head quartering (45°)	1.0	7.0
13	Beam sea (90°)	1.0	5.0
14	Beam sea (90°)	0.5	5.0
15	Beam sea (90°)	0.5	7.0
16	Aft quartering (135°)	1.0	5.0
17	Aft quartering (135°)	1.0	7.0
18	Following sea (180°)	1.0	5.0
19	Following sea (180°)	1.0	7.0

Table 5: Test conditions for DHI model tests load case 2

- Installation Load Case 3- This load case modelled the phase where GBS was resting on the seabed while the barge was still floating in between the legs of the GBS.

Test No	Wave heading	H_s (m)	T_p (s)
20	Head sea (0°)	1.0	5.0
21	Head sea (0°)	1.0	7.0
22	Head sea (0°)	2.0	7.0
23	Head quartering (45°)	1.5	7.0
24	Head quartering (45°)	1.0	5.0
25	Head quartering (45°)	1.0	7.0
26	Beam sea (90°)	0.5	5.0
27	Beam sea (90°)	0.5	7.0

Table 6: Test conditions for DHI model tests load case 3

With that, minimum and maximum values of displacement along with standard deviation values and mean values of displacement is generated for the surge, sway, heave, roll, pitch, and yaw of the barge and GBS. Minimum and maximum loads in the mooring and stretcher line are also obtained for each case load. All recorded data and the results are presented in the form of statistical data, time series and spectra.

2.5 Turkmenistan Oceanographic Data

Wave environment simulated by the wave generator will be based on oceanographic data recorded at Block 1 Fields, Caspian Sea. The Caspian Sea is the largest land locked body of water on the planet and is accessible through the Volga River via the Volga-Don Canal or Volga Baltic canals which connect the Sea of Azov and the Baltic Sea to the Caspian.[13] The Caspian weather is dominated by local geography and influences rather than by the traditional four seasons. The physical constraints of the Caspian and local weather conditions cause seas with a short period and limited height. Table 2, 3 and 4 below is a tabulation of the wave heights and periods at Block 1 fields with 1-year return period followed by 10 years and subsequently 100 years. For regular waves, I'll be mainly concerned with maximum wave height (H_{max}) and associated period (T_{ass}).

(a) RETURN PERIOD: 1 YEAR (from) Wave Criteria						
	North to Northeast	Northwest	East to Southeast	South	Southwest to West	All Directional
Significant Wave Height, Hs (m)	4.2	4.7	2.2	2.8	3.5	4.7
Zero Crossing Period, Tz (s)	7.3	7.7	5.7	6.3	6.8	7.7
Max. Wave Height, Hmax (m)	7.6	8.5	4.0	5.0	6.3	8.5
Associated Period, Tass (s)	10.6	11.1	8.3	9.1	9.9	11.1

Table 7: Block 1 Fields- Wave heights and periods for 1 year return period

(b) RETURN PERIOD: 10 YEAR (from) Wave Criteria						
	North to Northeast	Northwest	East to Southeast	South	Southwest to West	All Directional
Significant Wave Height, Hs (m)	5.7	6.3	2.7	2.8	3.8	6.3
Zero Crossing Period, Tz (s)	8.3	8.7	6.2	6.3	7.1	8.7
Max. Wave Height, Hmax (m)	10.3	11.3	4.9	5.0	6.8	11.3
Associated Period, Tass (s)	12.1	12.6	8.9	9.1	10.2	12.6

Table 8: Block 1 Fields- Wave heights and periods for 10 year return period

(c) RETURN PERIOD: 100 YEAR (from) Wave Criteria						
	North to Northeast	Northwest	East to Southeast	South	Southwest to West	All Directional
Significant Wave Height, Hs (m)	6.7	7.3	3.3	4.7	5.2	7.3
Zero Crossing Period, Tz (s)	8.9	9.2	6.7	7.7	8.0	9.2
Max. Wave Height, Hmax (m)	12.1	13.1	6.0	8.5	9.4	13.1
Associated Period, Tass (s)	12.9	13.4	9.7	11.1	11.6	13.4

Table 9: Block 1 Fields- Wave heights and periods for 100 year return period

2.6 Response Amplitude Operator (RAO) [14]

In my study, response of the barge structure when subjected to regular waves is described using the Response-Amplitude Operator (RAO) or Transfer Function, so called because it allows the transfer of the exciting waves into the response of the structure. In other words, it is used to determine the effect that a sea state will have upon the structure. It is often found in practice that an RAO is defined as response amplitude per unit wave height. RAO can also be defined as the amplitude or response per unit wave amplitude.

RAO could be theoretical or measured. The theoretical RAO's are obtained with the help of simplified mathematical formulas. By assuming the structure is restricted from motions and subjected to regular waves, forces acting on the body can be determined using:

- Froude-Krylov force, which is the pressure in the undisturbed waves integrated over the wetted surface of the structure
- Pressure Area method, which are pressures that occur due to disturbances in the water caused by presence of structure

When the problem is complicated to solve analytically or when the mathematical assumptions need verification such as the case of my final year project, tests are performed on a model of the prototype structure with regular waves in the controlled environment of the laboratory. The test results on model RAO's can then be scaled up to obtain prototype RAO's. Response function is generally constructed for a range of wave frequencies of interest for a given offshore structure, but that is in the case of random waves.

For regular waves where there is only one period along with one frequency, the response function at a single wave frequency can be written as:

$$\text{Response}(t) = (\text{RAO})\,\eta(t)$$

noting that $\eta(t) = (H/2)\cos(kx-wt)$ where $\eta(t)$ is the wave profile as a function of time, t.

CHAPTER 3

METHODOLOGY

For the research and investigation of this project, theoretical formulas required for numerical analysis will be gathered beforehand based on fundamental hydrodynamic concepts. Following that would be modelling tests using the fabricated barge model to determine the motion spectrum of the structure when subjected to waves. An overview of the activities for my Final Year Project can be found in APPENDIX A. From both numerical analysis and modelling tests, the respective RAO (Response Amplitude Operator) relating the dynamic motion of the barge to the wave-forcing function on the barge is determined. This chapter will attempt to provide a detailed explanation on method of derivation for both theoretical RAO from numerical analysis and measured RAO from model tests.

3.1 Modelling tests

3.1.1 Reference data

For model testing, model of the prototype barge used is based on a scale of 1:50, scaled down from the actual vessel used for ODP-A platform installation. As for the barge model's centre of gravity, it is located 161.7cm from the bow or 303.35cm from the forked stern. A plan view drawing of the scaled barge model is provided in Figure 10. Wave setup simulated for experimental purposes are also scaled down according to a 1:50 scale from the actual Turkmenistan conditions: The extent of the experiment covers 5 regular wave conditions as listed below:

	wave height (m)	wave period (s)	frequency (Hz)	
1				
2	0.0372	0.98	1.02	Regular
3	0.0372	1.12	0.89	
4	0.0372	1.26	0.79	
5	0.0372	1.40	0.714	

Table 10: Scaled down regular wave test conditions for model testing

However, due to limited time, I'll only be conducting tests using conditions highlighted above with wave height of 0.0372m, wave period of 0.84s and wave frequency of 1.19 Hz. This will thus be fixed as reference data for my study. However it is important to note that the list provided above is a scaled down tabulation of the selected condition. Provided below is a side to side comparison of the model and prototype reference data:

Parameter	Model	Prototype
Wave height (m)	0.0372	1.86
Wave period (s)	0.84	6
Wave frequency (Hz)	1.19	0.167
Water depth (m)	1.23	61.7
Barge draft (m)	0.08	4
Wave direction (^{0})	180	

Table 11: Breakdown of reference data used for model tests

The scaling between model and prototype is in reference to Froude-Krylov scaling whereby wave height, water depth and barge draft is a linear parameter therefore it is directly based on a 1:50 scale. However for wave period and wave frequency, these parameters are non-linear. Hence, it is calculated with regards to $\sqrt{50}$. For water depth, although it is calculated that model depth should be 1.23m, limitation of the wave tank at UTP's offshore laboratory meant that the depth had to be reduced to 1.0m. However, this difference of 0.23m is not significant to the experimental results.

3.1.2 Decay tests

Prior to the experiment, mass of the barge was weighed and determined to be 60kg. Decay tests have also been conducted to reveal the natural period and damping ratio of the barge structure in the concerned vessel motions direction. The respective natural period and damping ratio of the barge in the surge, heave and pitch direction are found out to be:

Condition	Barge
Surge Natural Period	78
Heave Natural Period	4887.12
Pitch Natural Period	43
Surge Damping Ratio	0.031847348
Heave Damping Ratio	0.05
Pitch Damping Ratio	0.234

Table 12: Natural period and damping ratio of barge structure

As observed in Table 12 above, natural period and damping ratio in the heave direction are abnormal. Due to overdamping in the heave direction, natural period and damping ratio could not be determined, thus assumed to be of a certain value based on DHI model test manual.

3.1.3 Model test details

Prior to the experiment, barge set up is to be positioned directly at the centre of the wave tank. A big portion of my study is revolved around parametric comparison and that is done mainly using numerical analysis. However, the analysis results must be validated via modelling tests.

Main aim of modelling tests has one aspect: determine dynamic responses of barge. Dynamic responses of barge to environmental loads are recorded using an optical tracking system with five bulb reflectors attached randomly onto the top of the barge model as shown in Figure 11. With the bulb reflectors, displacements along all degree of freedoms of the model can be recorded in relevance to a coordinate system. The recording of all 6 degrees of motion freedom on the other hand is done by three optical tracking cameras (Figure 12) by detecting the reflection of the bulbs. For my study however, only responses along the surge, heave and pitch of the model due to regular waves at a 180^0 direction will be analyzed.

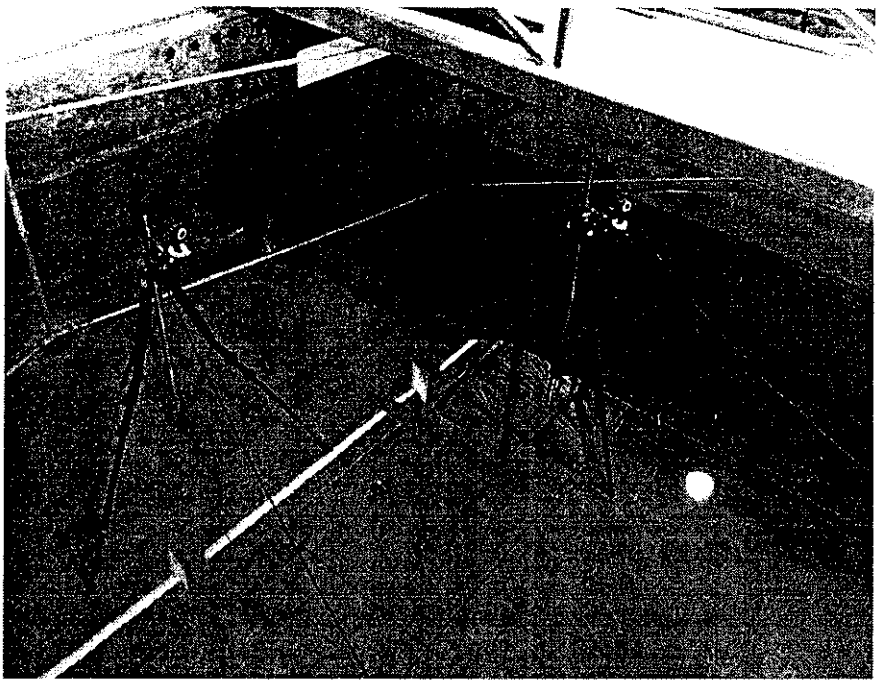

Figure 10: Optical tracking cameras

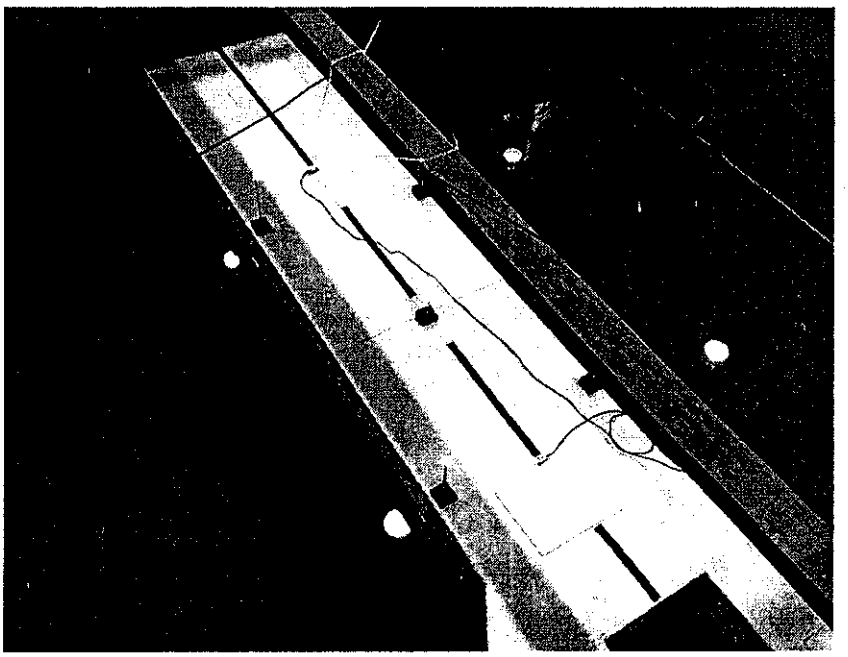

Figure 11: Bulb reflectors attached onto barge model

Meanwhile, load cells as seen in Figure 13 are attached to all 4 mooring lines hooked to the barge model edge (2 at the bow and 2 at the stern). With the load cells, tension in all mooring lines can then be calibrated to a precise 30 kN as

depicted in Figure 14. The tension stated above is again a scaled down force from the actual mooring line tension used in ODP-A platform installation. With the mooring lines, it simulates the restrained motions of barge and therefore a more accurate prediction of barge responses during floatover installation can be made.

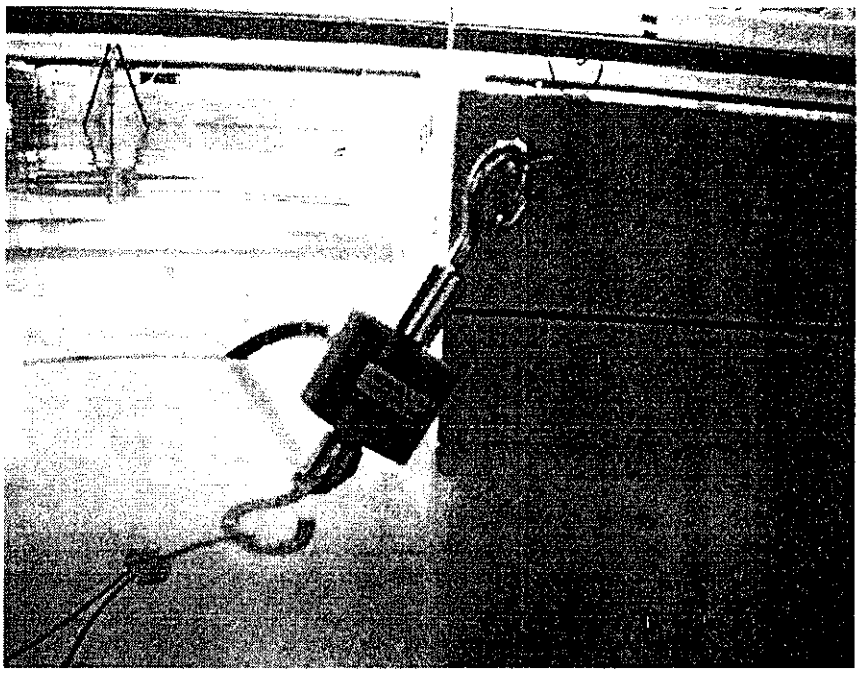

Figure 12: Load cells attached onto barge stern

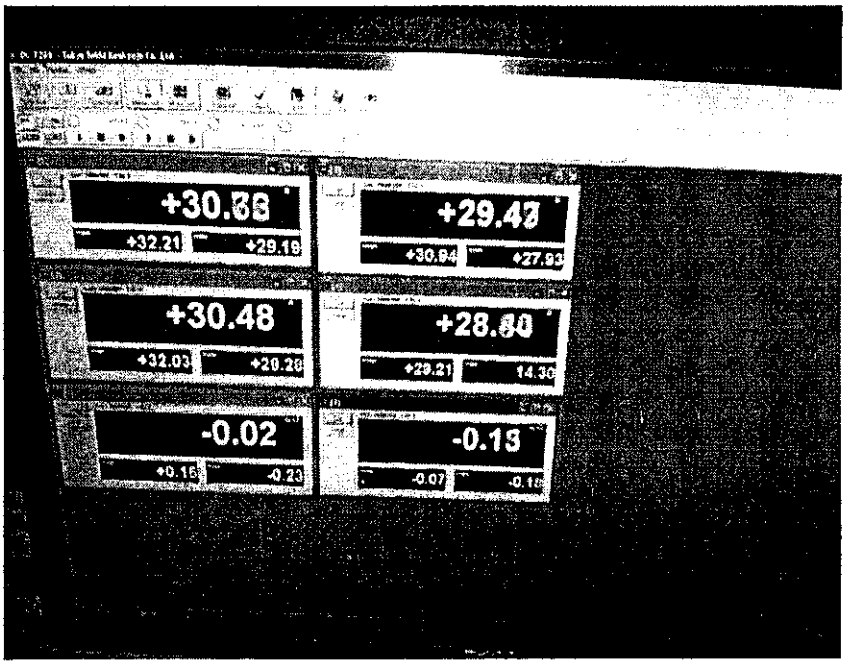

Figure 13: Tension at mooring lines calibrated to 30 kN

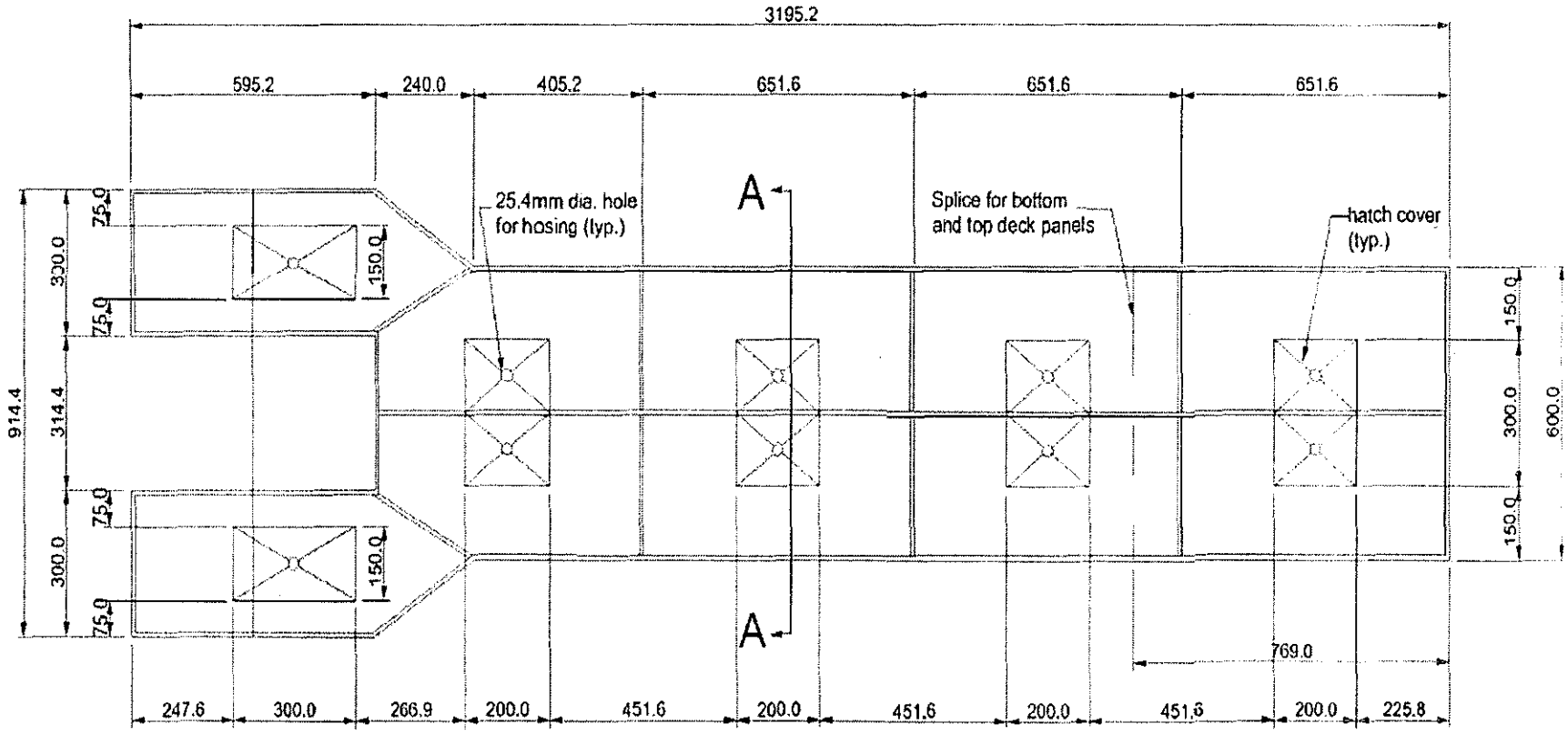

Figure 14: Plan view of the 1:50 scaled barge model

3.2 Numerical Analysis

3.2.1 Linear Airy wave theory

As clearly shown in the Froude-Krylov force formula in Section 3.2.2 the calculations are mainly concerned with water particle accelerations. The simplest and most useful of all wave theories – the small amplitude wave theory or better known as linear airy wave theory is thus used to calculate particle accelerations.

Acceleration:

$$\dot{U}_o = \frac{2\Pi^2 H}{T^2}\frac{\cosh ks}{\sinh kd}\sin\Theta$$

$$\dot{V}_o = \frac{2\Pi^2 H}{T^2}\frac{\sinh ks}{\sinh kd}\cos\Theta$$

3.2.2 Force calculation

Numerical analysis will be done mainly using Microsoft Excel spreadsheets. This portion of the project is largely based on Froude-Krylov force equation for Rectangular Block. The horizontal force, F_x is assumed as surge while vertical force, F_y is taken as heave.

$$F_x = C_H \rho V \frac{\sinh(\frac{kL_3}{2})}{kL_3/2}\frac{\sinh(\frac{kL_1}{2})}{kL_1/2}\dot{U}_o$$

$$F_y = C_V \rho V \frac{\sinh(\frac{kL_3}{2})}{kL_3/2}\frac{\sinh(\frac{kL_1}{2})}{kL_1/2}\dot{V}_o$$

Finite element approach is applied in theoretical calculations whereby the barge is divided up into units of 1m. With that, forces acting on the middle of each units in the x and y direction are determined using formula stated above. Summation of all the forces in the x direction will be taken as the total horizontal force and y direction for vertical force.

For force in the surge (horizontal) direction however, the analysis is also concerned with water draft depth. Take for instance, with the reference data of 4m water draft. The draft depth will be divided into equal units of 1. Total forces at each unit length of the barge will be determined at the middle depth of all 4 water draft units. In other words, surge force calculation for 4m draft would result in 4 different forces at 4 different water draft depths. The summation of these 4 forces equals to the total horizontal force on the barge.

Force in the pitch direction is a moment force determined from multiplying each individual unit forces in the x and y direction by moment arm (distance from centre of gravity to point on unit undergoing torque). Summing up the moment force in all units would result in M_x and M_y, both pertinent in the calculation of pitch force.

3.2.3 Parametric comparison

As mentioned in the scope of study, parametric comparison is achieved by manipulating a few parameters: water depth, water draft, wave period, wave direction and mooring line stiffness. Data for water depth and wave period are based on 4 locations in Malaysian seas (PMO, Balingian, Baram Delta, and Samarang). All information is in accordance to latest PETRONAS technical standards for Malaysian operation.

- PMO (Water depth = 70m)

WAVE [1]		
H_s	m	*4.38* [1]
T_z	sec	*6.91*
T_p	sec	*9.74*
H_{max}	m	*8.44*
T_{ass}	sec	*8.38*

Table 13: Operating criteria at PMO

- Balingian (Water depth = 30m)

WAVE		
H_s	m	3.1
T_z	sec	7
T_p	sec	9.8
H_{max}	m	5.8
T_{ass}	sec	9

Table 14: Operating criteria at Balingian

- Baram Delta (Water depth = 75m)

WAVE		
H_s	m	3.3
T_z	sec	6.7
T_p	sec	9.6
H_{max}	m	6.5
T_{ass}	sec	8.9

Table 15: Operating criteria at Baram Delta

- Samarang (Water depth = 50m)

WAVE		
H_s	m	3.7
T_z	sec	7.2
T_p	sec	10.1
H_{max}	m	6.9
T_{ass}	sec	9.4

Table 16: Operation criteria at Samarang

As for water draft, three values are set- 2m, 4m and 6.75m. Wave direction on the other hand, I'll only be comparing the difference in response when subjected to a 0^0 and 180^0 wave heading. For the mooring line stiffness parameter, investigation is done to determine how barge responses to a stiffness increment of 20% , 40% and decrement of 20%, 40%.

When studying the effects of water depth on barge motions for instance, all other variables are fixed as reference data value. To put it simply, only the water depth parameter varies but other parameters will be set at the conditions for reference data. By doing so, the motion response for different water depth can be plotted against time to determine whether a change in water depth causes a resonating

change in barge motions. This is likewise when studying the effects of change in water draft, wave period, wave direction or mooring line stiffness. Table 17 shows a tabulation of each parameter along with the highlighted control data:

Water depth (m)	Wave period (s)	Wave direction (°)	Mooring line stiffness	Barge draft (m)
30	6	0	Original	2
50	8.38		+ 20%	
61.7	8.9		+40%	4
70	9	180	-20%	
75	9.4		-40%	6.75

Table 17: Tabulation of data used for parametric comparison

Table 18 below further illustrates the manipulation of mooring line stiffness for the surge, heave and pitch direction

	Original	+ 20%	+ 40%	- 20%	- 40%
Surge	0.1313568	0.15762821	0.18389958	0.10508547	0.07881410
Heave	48.405538	58.0866457	67.7677533	38.7244308	29.0433228
Pitch	944.48766	1133.38519	1322.28273	755.590132	566.692599

Table 18: Data used for parametric comparison of mooring line stiffness

3.3 Results presentation

3.3.1 Theoretical RAO

From numerical analysis, the theoretical RAO can be determined using the function written as:

$$RAO = \left[\frac{\frac{F_I}{\frac{H}{2}}}{[(K - m\omega^2)^2 + (C\omega^2)^2]^{\frac{1}{2}}} \right]$$

whereby F_I value is taken as the force calculated from Froude Krylov equation mentioned at the beginning of Chapter 3.2. Note that the F value has to be the maximum force applied onto the barge from a time of 0 to 6s (Wave period, T=6s). Substituting the maximum horizontal force, F_x would determine the motion RAO in the surge direction whereas maximum vertical force, F_y determines RAO in the heave direction. For pitch RAO, the maximum moment force is taken as F_I parameter.

With the RAO values known in the surge, heave and pitch direction, the responses can thus be calculated using the formula below whereby H_{max} = 1.86m.

$$RAO_{surge,heave,pitch} = \frac{H_{surge,heave,pitch}}{H_{max}}$$

By plotting the responses against time using $\eta(t) = (H/2) \cos (kx-wt)$ simplified to be $\eta(t) = (H/2) \cos wt$, I can then arrive at the response profile. The profile plotted for each data in a single parameter will then be compared against each other, thus providing a clear picture of how each parameter affects barge motions.

3.3.2 Measured RAO

Referring to Figure 16, the total response spectrum, $S_F(\omega)$ or dynamic motion spectrum is written relating the response amplitude operators (RAO) to the wave energy spectrum, $S(\omega)$ using the formula listed below:

$$S_F(\omega) = [RAO]_F{}^2 S(\omega)$$

With model testing, the wave energy spectrum is recorded by wave probes located at the end of the water tank facility whereas motion spectrum is determined from the Optical Tracking System. Therefore by using the formula shown above, the measured motion RAO can be easily derived. As explained earlier, purpose of model tests are only to validate or justify theoretical results. Thus, in my study, comparison of experimental and theoretical results is only done for the reference data.

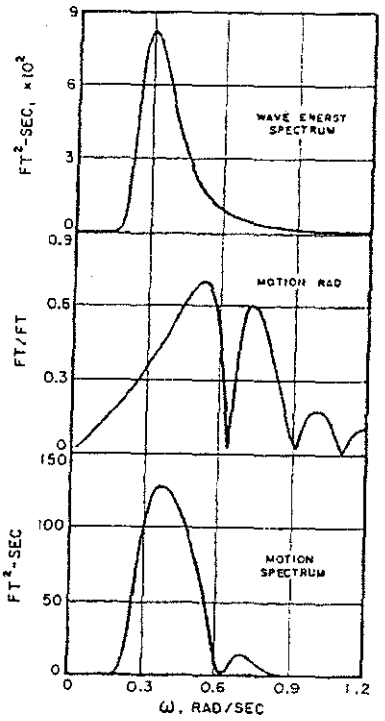

Figure 15: Resulting spectrums from model test

3.4 Tools required

This study involves modelling tests and theoretical analysis. Main instruments required for the modelling include:

1. Wave generator
   - For generation of waves based on Turkmenistan oceanographic data input
2. Wave probe
   - To record the wave characteristics after encounter with barge model
3. Velocimeters and Accelerometers
   - To record velocity and acceleration of the test wave's water particles
4. Load cells
   - To measure the tension in each mooring line.
5. Optical tracking system
   - To detect the motions of the barge model

Whereas for theoretical analysis, main requirement is software application as stated below:

1. Microsoft Excel
   - To develop calculation spreadsheets

CHAPTER 4

RESULTS AND DISCUSSION

4.1 Varying water depth

Surge

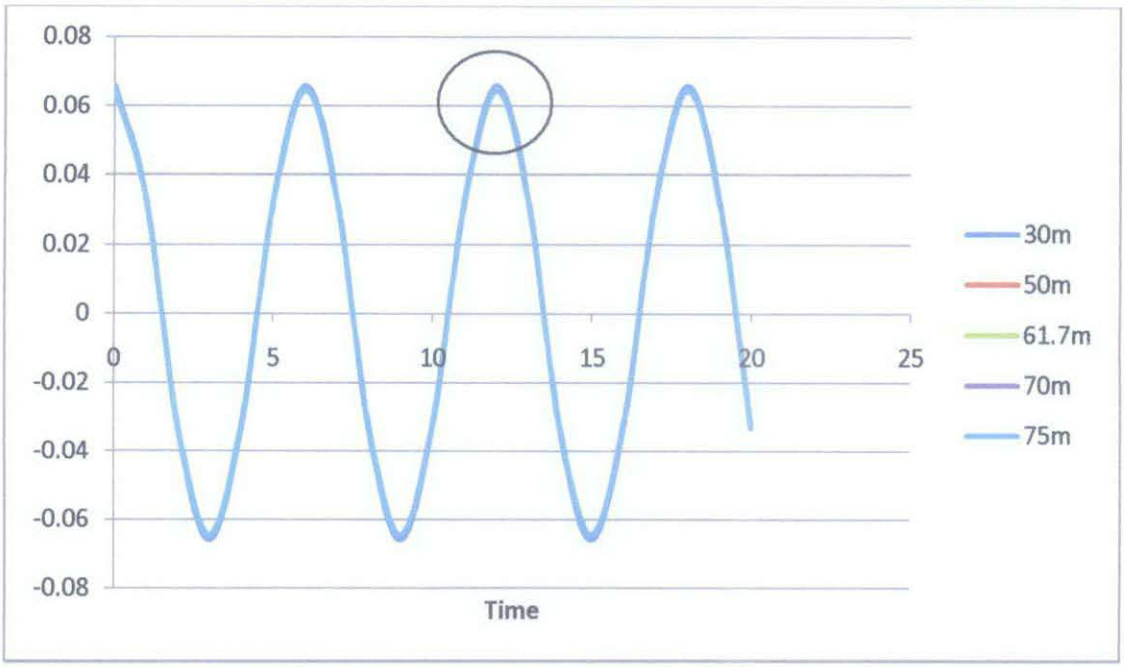

Zooming in on the plot yields:

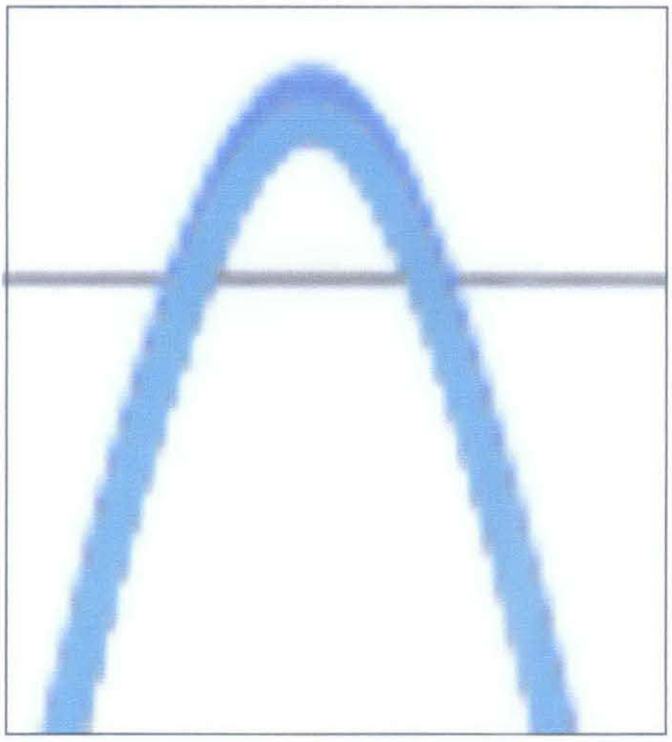

Water depth	30	50	61.7	70	75
Max F_x	1.454405294	1.427043215	1.426719473	1.426718783	1.426718697
RAO	0.070865562	0.069532352	0.069516577	0.069516544	0.069516539
H_{surge}	0.131809946	0.129330174	0.129300834	0.129300771	0.129300763

Through the plots, it can be deduced that water depth has minimal to no effect on barge motions. Varying the parameter yields no significant change in the responses. This is naturally so because the barge is a floating structure. In calculation of force on any offshore structure, force is assumed to be composed of inertia and drag forces. However, in the case of a floating structure inertia force predominates over drag force and that is why Froude-Krylov force is applied instead of Morison equation as Morison assumes inertia and drag to be linearly added together. Water depth is only relevant when the drag force is being considered hence for a floating structure like the floatover barge, water depth has no effect on barge motions. Nonetheless, further investigation into the RAO values presented above shows that there are variations in value when water depth varies, but only within the range of 0.00003 to 0.003 which can be deemed insignificant. Zooming in on the plot also revealed that there is a slight difference between the 5 plots. But, there is a trend – the shallower the water is, the higher the RAO or motion responses. Waves propagating towards shallow region tend to slow down due to friction with the seabed, resulting in a longer period (shorter wave frequency). Referring to the RAO formula shown below, it is clear that wave frequency, ω has an inverted relationship with RAO thus explaining how a shorter wave frequency as a result of shallow water depth leads to higher RAO.

$$RAO = \left[\frac{\frac{F_I}{\frac{H}{2}}}{[(K - m\omega^2)^2 + (C\omega^2)^2]^{\frac{1}{2}}} \right]$$

Pitch

Water depth	30	50	61.7	70	75
Max F_x	463.014485	462.8188001	462.8130764	462.8140964	462.8142236
RAO	0.010443811	0.010439398	0.010439268	0.010439291	0.010439294
H_{pitch}	0.019425489	0.01941728	0.019417039	0.019417082	0.019417088

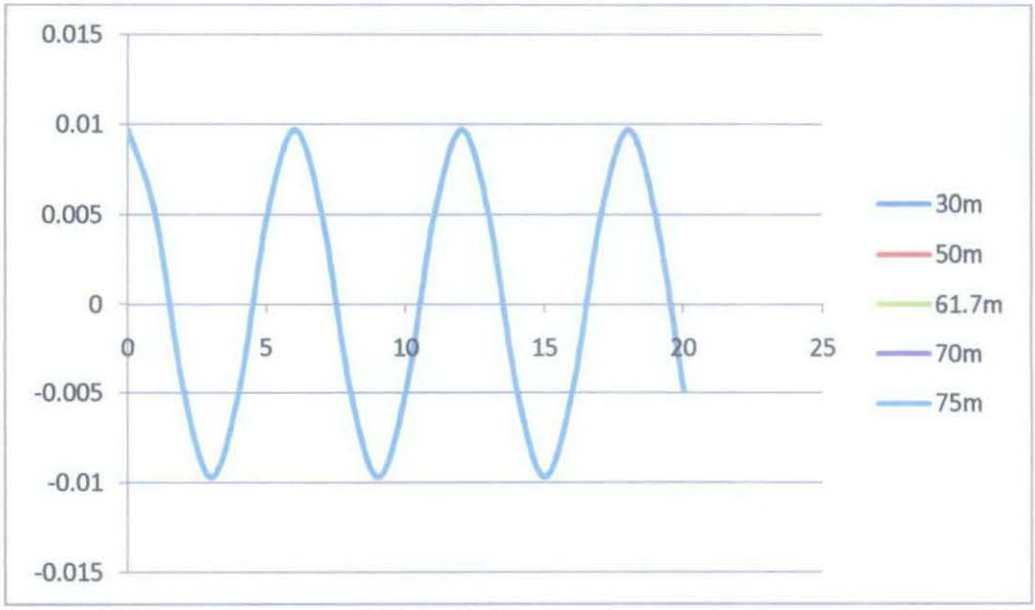

A similar trend can also be said for the effects of water depth on motions in the pitch direction, whereby it can be considered insignificant.

Heave

Water depth	30	50	61.7	70	75
Max F_x	5.809354762	5.779252598	5.778854691	5.7788674	5.778868984
RAO	0.911226462	0.906504787	0.906442373	0.906444366	0.906444615
H_{heave}	1.69488122	1.686098903	1.685982814	1.685986522	1.685986984

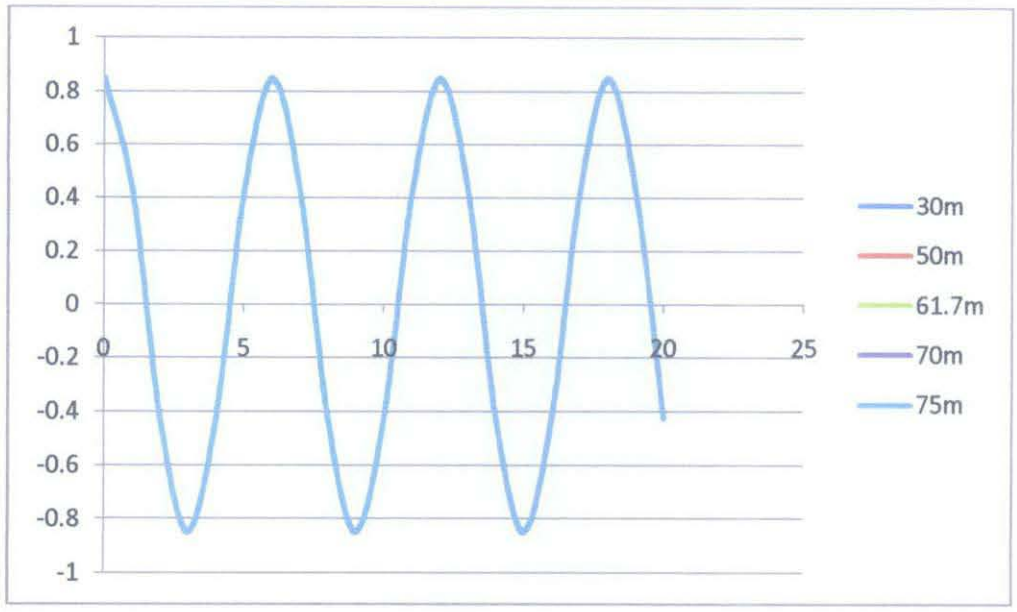

For motion responses in the heave direction, water depth also has insignificant effect as per surge and pitch direction. What differs is how the RAO values fluctuates however minimal to the variation in water depth. For heave and pitch, responses do not decline as water depth increases. In fact, RAO is at its lowest around the depth of 62m and is then on an increasing trend as water becomes deeper. This can be accounted to the reason being that wave movement is parallel to the surge direction thus causing a linear response whereas creating a non-linear movement for the heave and pitch direction.

Detailed calculation of RAO for varying water depth is attached in APPENDIX B.

4.2 Varying barge draft

Surge

Barge draft	2m	4m	6.75m
Max F_x	0.792799656	1.426719473	2.025914781
RAO	0.077820233	0.069516577	0.058067779
H_{surge}	0.144745634	0.129300834	0.108006069

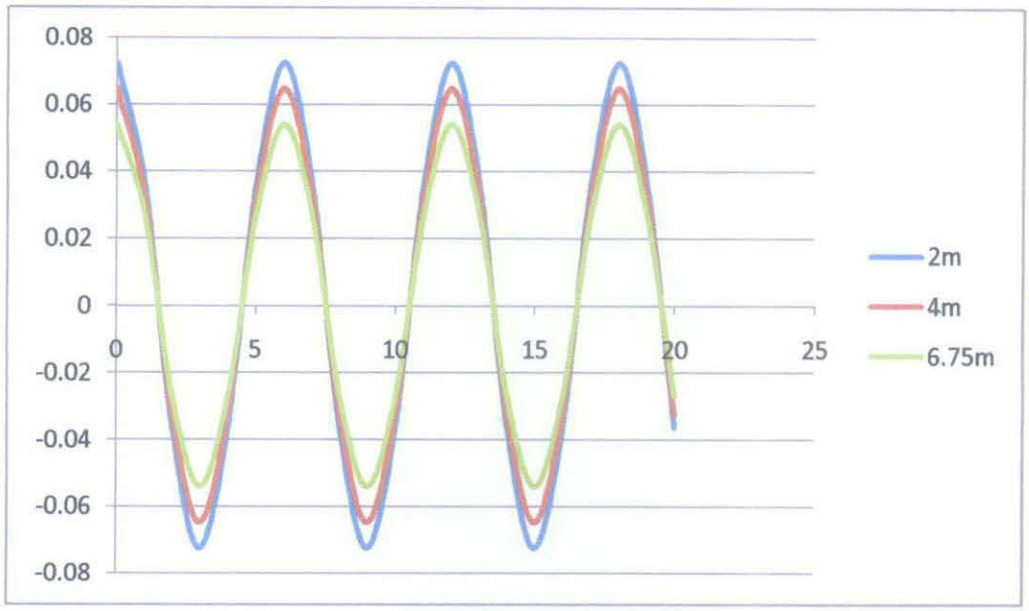

Amongst all parameters, barge draft is identified to have the most effect on barge motions as exhibited by the response profile shown above. The draft has a direct correlation to the mass of the barge, in the sense that a higher draft means the barge weighs more. Therefore, with a larger mass, the barge is able to stabilize itself against the wave elements thus leading to more controlled responses. In other words, lower RAO as proven by the results above.

Pitch

Barge draft	2m	4m	6.75m
Max F_x	256.9599603	462.8130764	680.1688192
RAO	0.011757858	0.010439268	0.008962492
H_{pitch}	0.021869615	0.019417039	0.016670235

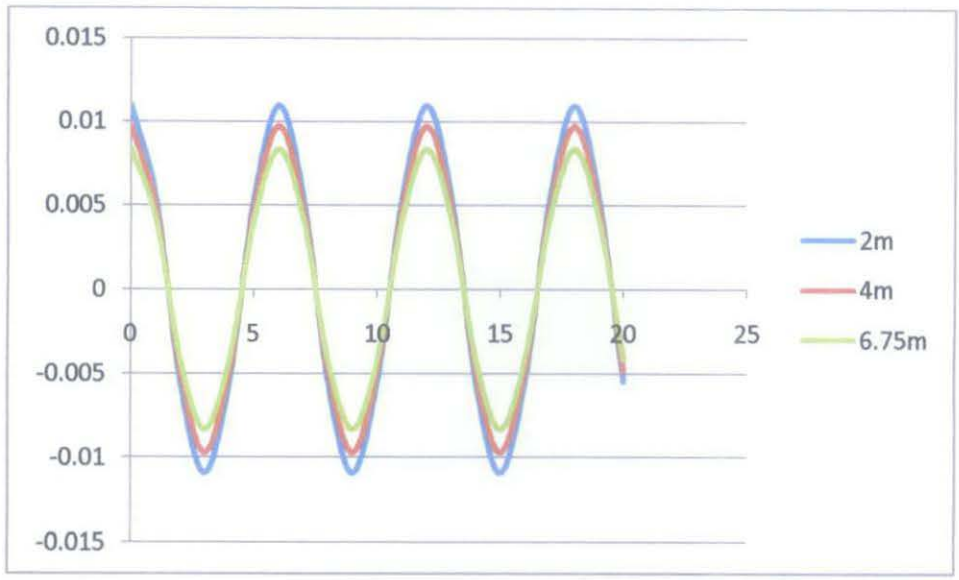

Motion responses in the pitch direction has also exhibited similar pattern whereby larger draft yields a lower RAO.

Heave

Barge draft	2m	4m	6.75m
Max F_x	3.211196747	5.778854691	8.490939139
RAO	0.128127112	0.906442373	0.359794777
H_{heave}	0.238316428	1.685982814	0.669218285

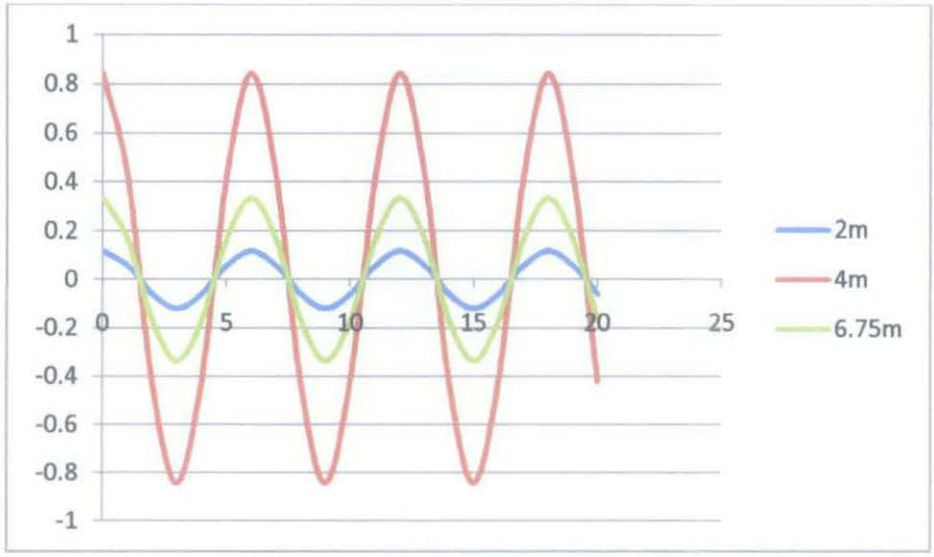

In the heave direction, theoretical analysis results are completely not in accordance to the relation between barge draft and RAO. The larger the draft, the smaller the RAO- this is a relationship that is not only established via theoretical

results completed for surge and pitch but also validated via modelling tests trend done by Masters students. The main reason being that natural period in the heave direction could not be determined precisely due to overdamping. Therefore, plenty of assumptions had to be made regarding these aspects, creating a situation where the wave period is near to the barge natural period as shown in the calculations below. This simply implies that the wave motions are calculated to be critical near the resonance of the structure thus leading to dynamic amplification. However, dynamic amplification factor is not taken into consideration in the Froude-Krylov equations. Thus, clearly explaining why RAO for certain drafts might be intensified in the heave direction.

Draft	Weight (M.kg)	Added Mass(M.kg)	Total mass (M.kg)	Stiffness,K
2.00	**9.8719824**	**9.8719824**	**19.7439648**	**48.4055381**
4.00	**19.7439648**	**19.7439648**	**39.4879296**	**48.4055381**
6.75	**33.3179406**	**33.3179406**	**66.6358812**	**48.4055381**

For 2m draft, barge natural frequency = $\sqrt{\frac{k}{m}} = \sqrt{\frac{48.4055381}{19.7439648}} = 1.57\ rad/s$

Therefore, barge period, $T_n = \frac{2\pi}{1.57} = 4.0s$

For 4m draft, barge natural frequency = $\sqrt{\frac{k}{m}} = \sqrt{\frac{48.4055381}{39.4879296}} = 1.11\ rad/s$

Therefore, barge period, $T_n = \frac{2\pi}{1.11} = 5.7s$

For 6.75m draft, barge natural frequency = $\sqrt{\frac{k}{m}} = \sqrt{\frac{48.4055381}{66.6358812}} = 0.85\ rad/s$

Therefore, barge period, $T_n = \frac{2\pi}{0.85} = 7.4s$

Calculations above clearly show how close barge period in the heave direction is to wave period of 6s. To rectify this error, alternative methods were explored. The Pressure Area method explained in Section 4.7 returned improved results but still was unable to generate desired outcome.

Detailed calculation of RAO for varying barge draft is attached in APPENDIX C.

4.3 Varying wave period

Surge

Wave period	6	8.38	8.9	9.0	9.4
Max F_x	1.42671947	3.028945983	2.699037524	2.5664172	1.761763683
RAO	0.06951657	0.289525146	0.291436328	0.283462906	0.212529386
H_{surge}	0.12930083	0.538516771	0.542071571	0.527241004	0.395304657

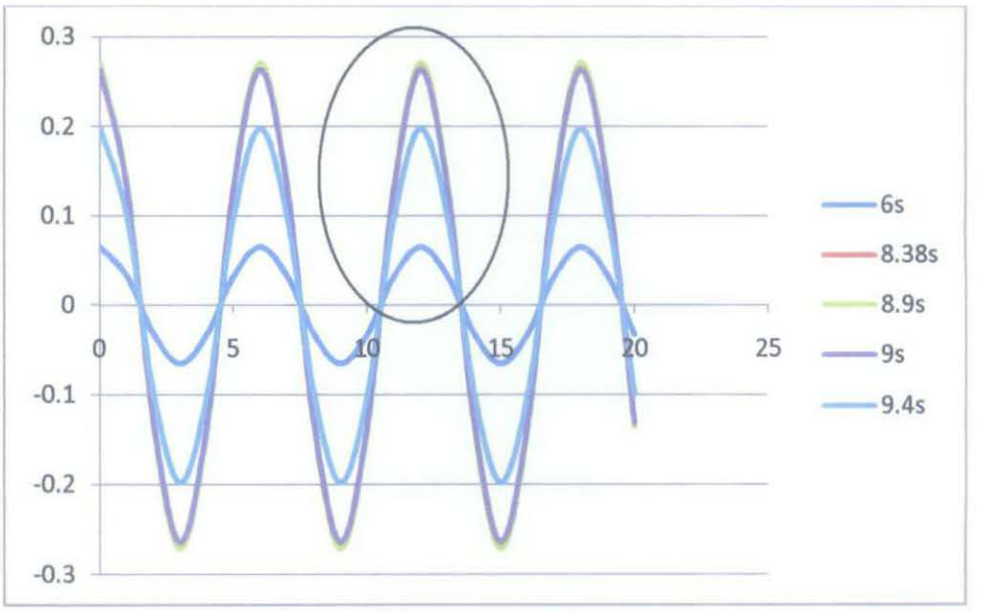

Zooming in on plot yields:

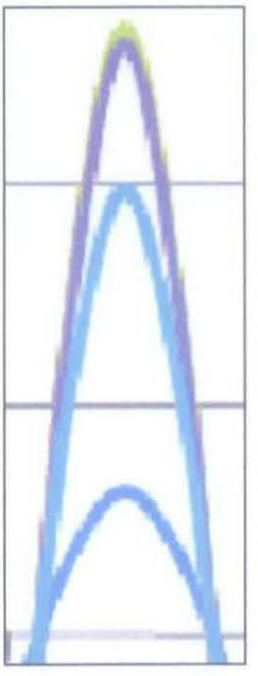

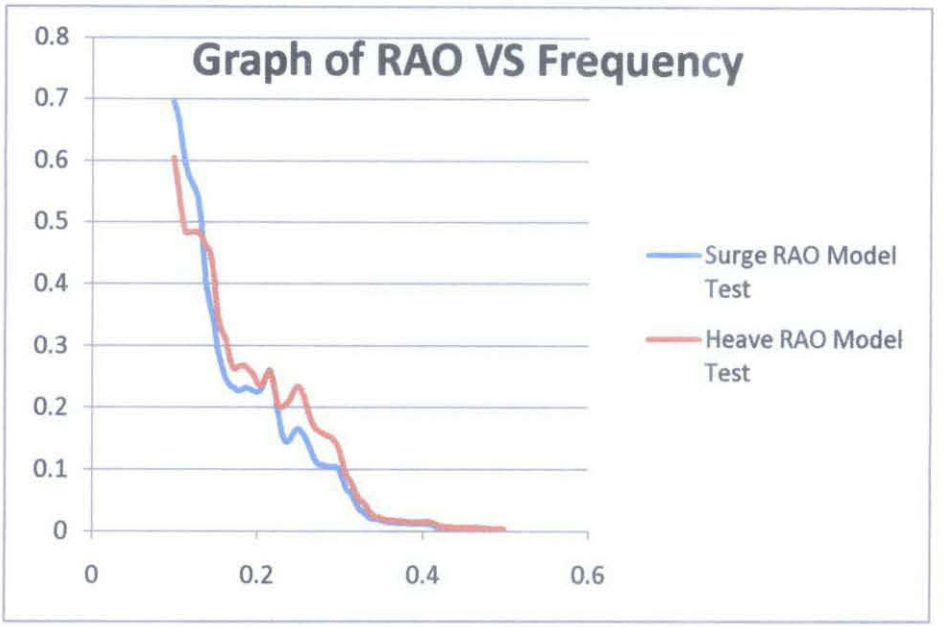

To truly explain the motion response patterns as wave period varies, reference has to be made to the graph of RAO vs frequency for random waves which follows a trend as shown above. For a longer wave period, that means a shorter frequency. As observed in the supplementary graph provided, RAO is peaked within the range of shorter frequency. That is why for longer wave period of 8.38, 8.9, 9.0 and 9.4s, the responses are relatively larger than that of a shorter wave period (6s). Based on that argument, wave period of 9.4s should then render the highest value of RAO. However, that is not the case. Again referring to the graph of RAO vs frequency, the responses does not behave in a linear mode but goes through a somewhat erratic pattern of up and down fluctuations. Thus, escalating wave periods don't necessarily mean increasing RAO. Take for instance from a wave period of 8.38 to 8.9 to 9.0 and then to 9.4 with RAO of 0.2895, 0.2914, 0.2835, 0.2125 respectively, it is obvious that motions follow an up and down fluctuation pattern as wave period varies.

Pitch

Wave period	6	8.38	8.9	9.0	9.4
Max F_x	462.8130764	705.5053724	640.3412447	635.7369418	569.6288919
RAO	0.010439268	0.031567843	0.032462196	0.032986334	0.032359783
H_{pitch}	0.019417039	0.058716188	0.060379685	0.061354582	0.060189196

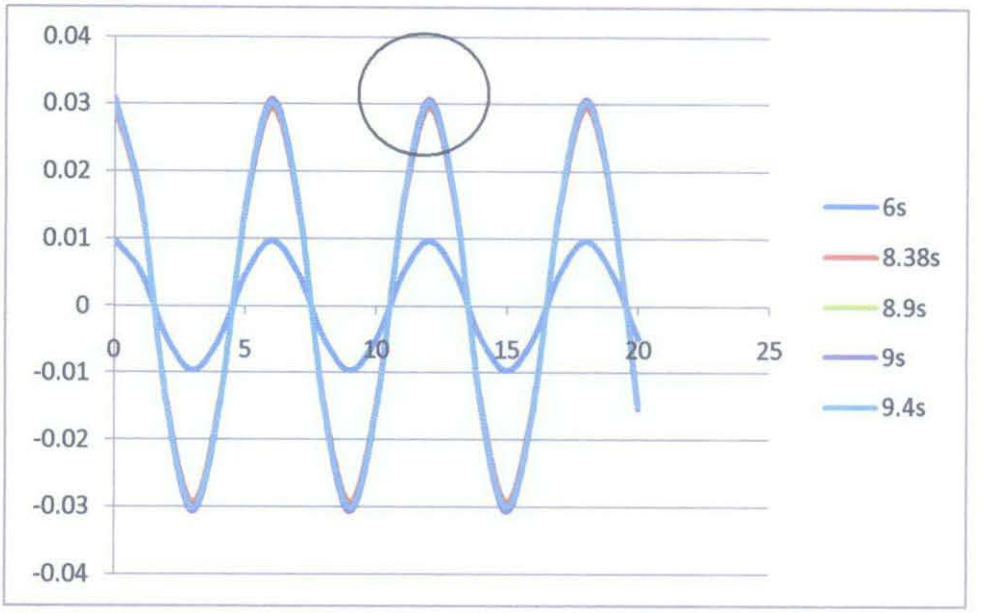

Zooming in on the plot yields:

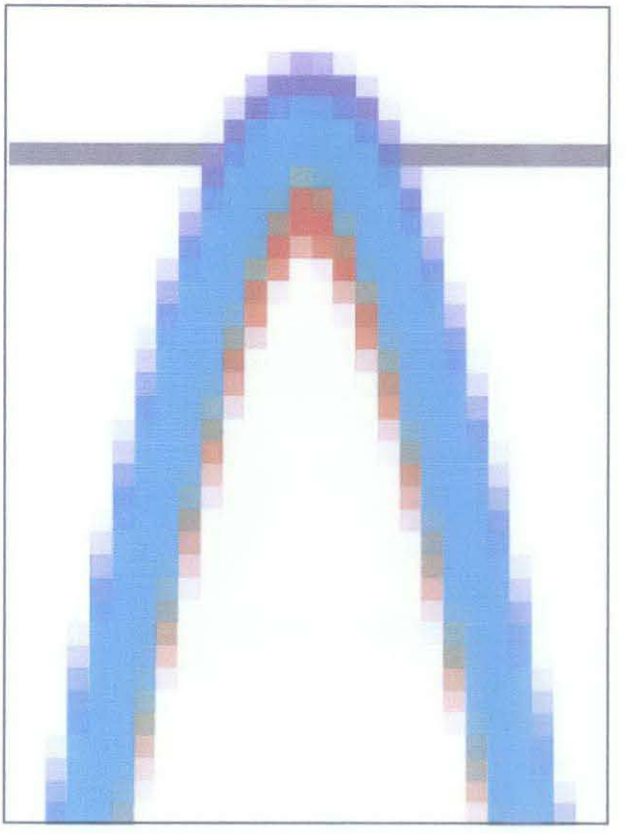

When wave period varies, more responses are observed in the pitch direction for a longer wave period (shorter wave frequency) as explained in Section 4.3. With the zoomed in version of the plot, it is evident that the response profile also follows the up and down fluctuation pattern, in accordance with the patterns observed for

motions in the surge direction only with the acceptance that these fluctuations are so minimal that the plots for different wave periods cannot be distinguished from one another. Nonetheless, the values reveal that the patterns are still there.

Heave

Wave period	6	8.38	8.9	9.0	9.4
Max F_x	5.778854691	11.95397987	10.44500993	10.00931549	7.169781527
RAO	0.906442373	0.486688274	0.388756753	0.367090914	0.249486859
H_{heave}	1.685982814	0.90524019	0.72308756	0.682789101	0.464045557

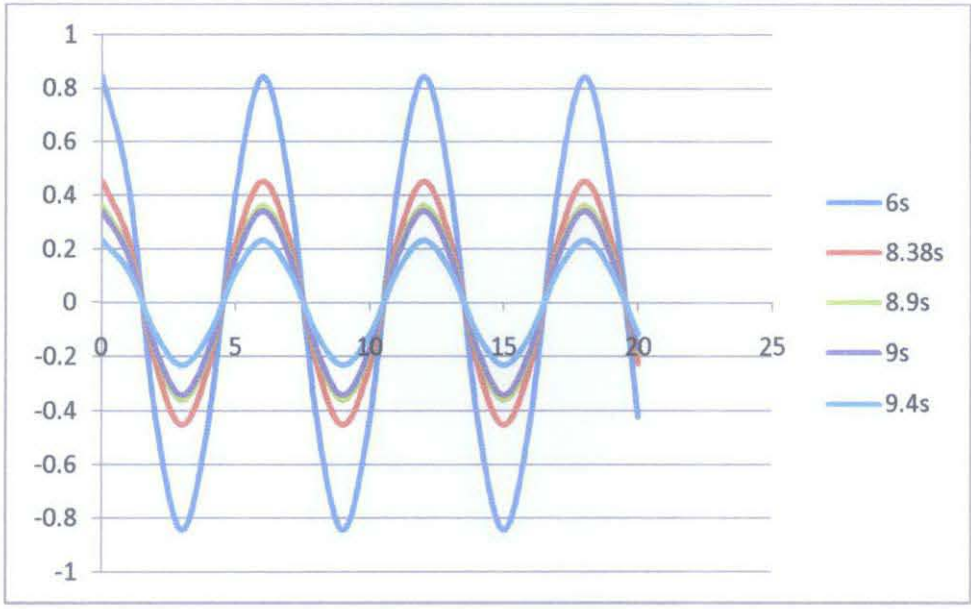

As per mentioned in Section 4.2 whereby dynamic amplifications exist due to the close range between barge natural period and wave period, the expected response when wave period varies thus cannot be observed in the heave direction. The directly inverse relationship between RAO and wave period does not correlate with the standard pattern exhibited when RAO is plotted against frequency. Please refer to Section 4.7 for the results obtained using another method known as the Pressure Area method.

Detailed calculation of RAO for varying barge draft is attached in APPENDIX D.

4.4 Varying mooring line stiffness

Surge

	0.131356843	0.157628212	0.18389958	0.105085475	0.078814106
Max F_x	1.426719473	1.426719473	1.426719473	1.426719473	1.426719473
RAO	0.069516577	0.069599262	0.069682144	0.069434088	0.069351794
H_{surge}	0.129300834	0.129454628	0.129608787	0.129147404	0.128994337

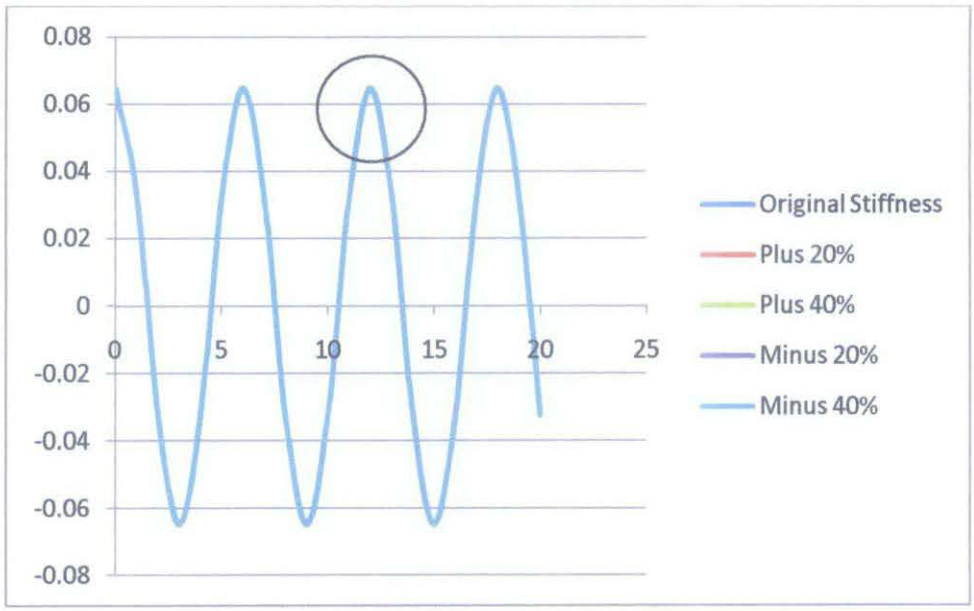

Zooming in on plot yields:

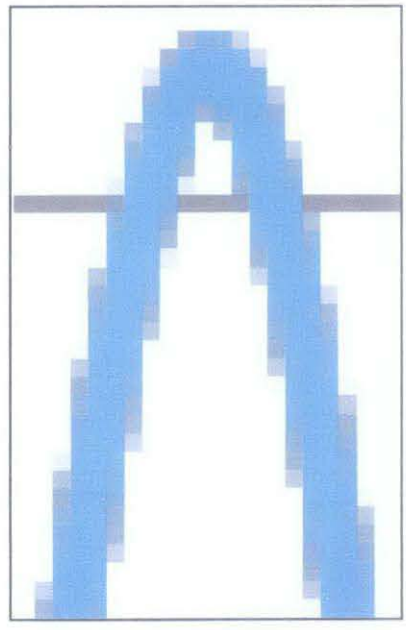

The mooring consists of a combination of equipment that is sized to suit the vessel motion characteristics, jacket rigidity and environmental conditions of the site. Mooring lines are generally designed to serve one function, which is to control the barge motions. A stiff mooring line does keep a better control of the vessel's position and maintain the second order wave induced motions of the vessel to a lower level (lower RAO). However, a stiffer mooring line also means a reduction in the effect of flexibility and increment in the tension of the mooring lines. At a certain point, the tension created might lead to high frequency oscillations (in the wave frequency range) that can generate significant dynamic amplification of the barge motions.[15] That could explain why results show that a stiffer mooring line yields a higher response (RAO) as opposed to a lower one as expected. Although the values are in line with the aforementioned theory, an addition and reduction of 20% and 40% to the mooring line stiffness does not affect the RAO distinctly enough to be translated onto the motion profile. But nevertheless, the zoomed in plot revealed a slight difference.

Pitch

	944.487666	1133.385199	1322.282732	755.5901328	566.6925996
Max F_x	462.8130764	462.8130764	462.8130764	462.8130764	462.8130764
RAO	0.010439268	0.010480707	0.010522474	0.010398156	0.010357366
H_{pitch}	0.019417039	0.019494114	0.019571802	0.01934057	0.0192647

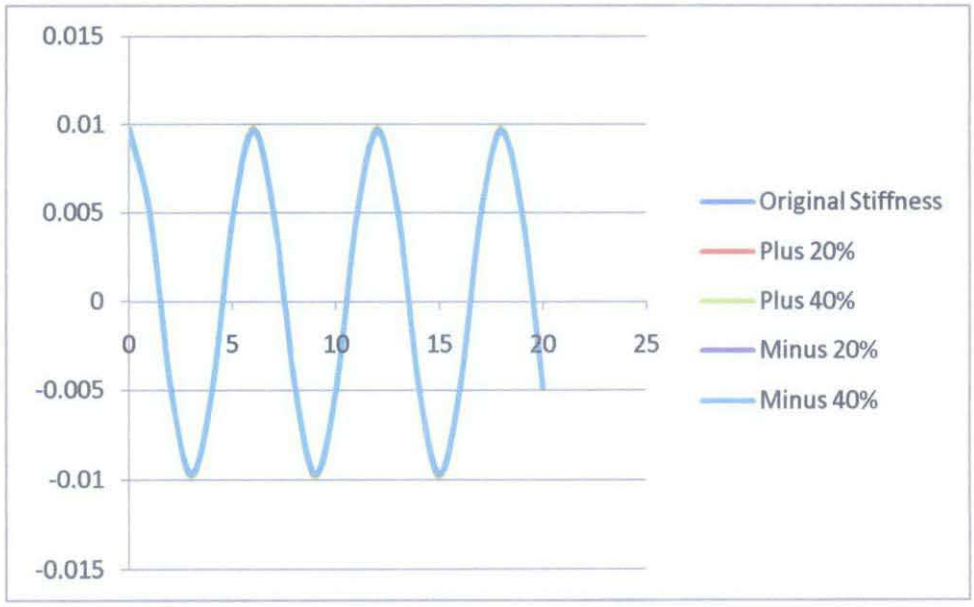

Motions in the pitch direction follow the same pattern as that of responses in the surge direction when mooring line stiffness was varied. Please refer to Section 4.4.1 for further explanation.

Heave

	48.4055381	58.08664572	67.76775334	38.72443048	29.04332286
Max F_x	5.778854691	5.778854691	5.778854691	5.778854691	5.778854691
RAO	0.906442373	0.398044803	0.247987679	1.011540595	0.422870076
H_{heave}	1.685982814	0.740363333	0.461257082	1.881465506	0.786538341

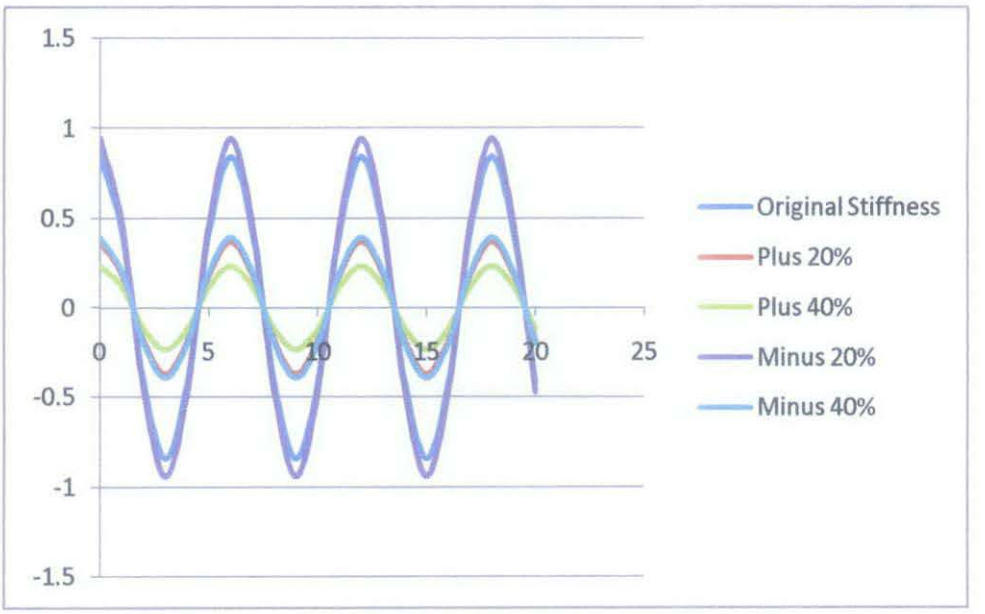

Jameel & Gupta (2000) conducted research on barge responses during Hurricane Georges and arrived at the conclusion that damping induced by mooring lines explains the very low level of heave responses as compared to motion in other directions. [16] Hence, it is safe to assume that mooring lines have a more considerable effect on restricting motions in the heave direction. Results of my study reflected such phenomena where a stiffer mooring line is more efficient in reducing heave motions as compared to surge and pitch direction. RAO value decreases with percentage increase of stiffness with the exception of stiffness = 29.04332286 MN/m (minus 20%) but this again can be attributed to dynamic amplification factors in the heave direction.

That said, although assumptions are being made to explain the responses in surge, heave and pitch direction when mooring line stiffness varies, this is all based theoretically. To truly prove such assumptions and verify their accuracy, modelling tests must be conducted to assure that experimental trends are in line with theoretical ones.

Detailed calculation of RAO for varying barge draft is attached in APPENDIX E.

4.5 Varying wave direction

Surge

Wave direction	180^0	0^0
Max F_x	1.426719473	1.400307444
RAO	0.069516577	0.068229657
H_{surge}	0.129300834	0.126907162

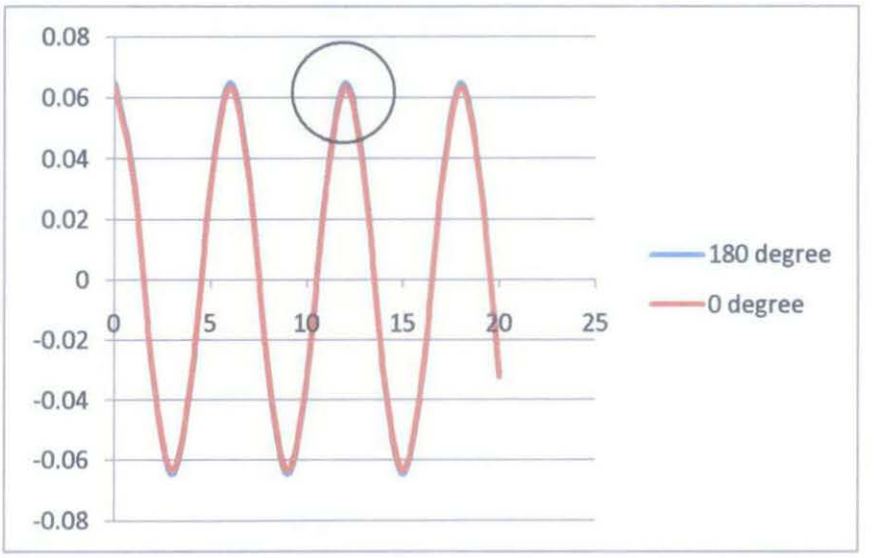

Zooming in on plot yields:

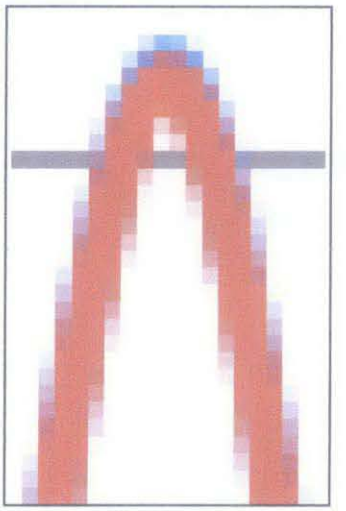

Pitch

Wave direction	180^0	0^0
Max F_x	462.8130764	452.0092489
RAO	0.010439268	0.010195576
H_{pitch}	0.019417039	0.018963771

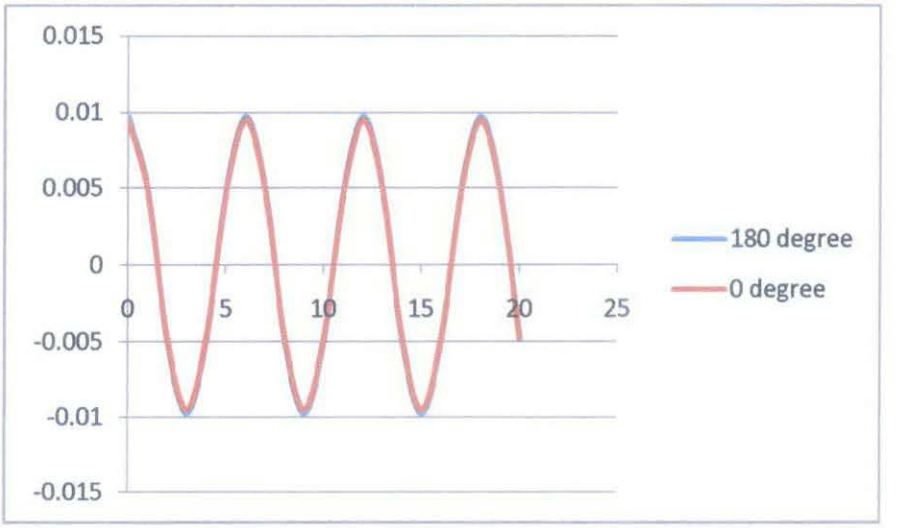

Heave

Wave direction	180^0	0^0
Max F_x	5.778854691	5.663871575
RAO	0.906442373	0.888406694
H_{heave}	1.685982814	1.652436451

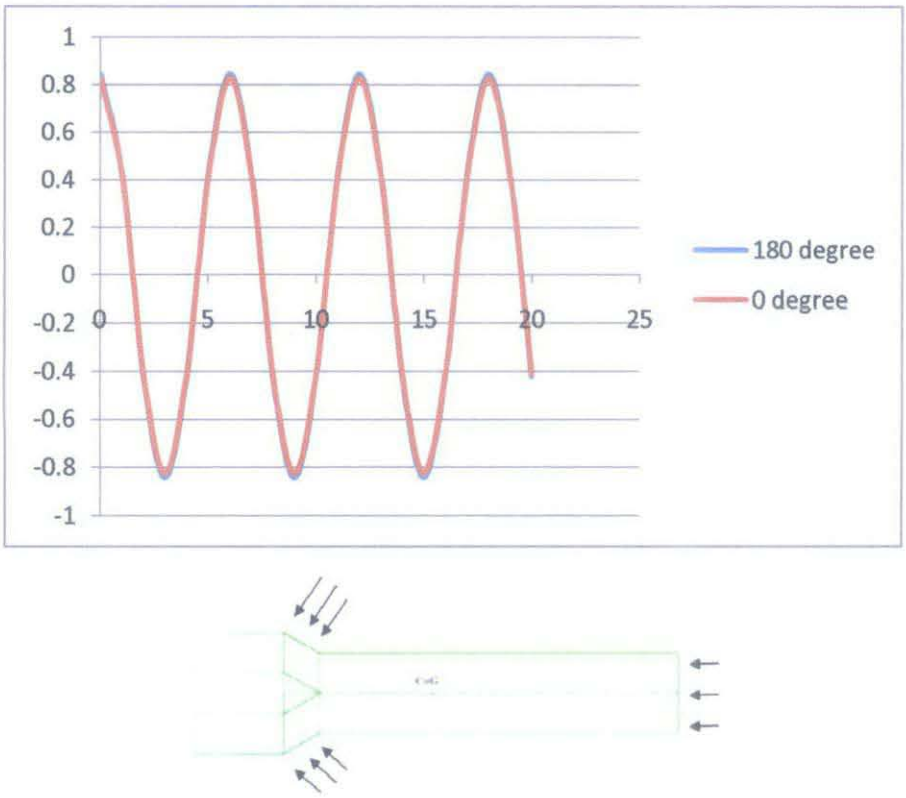

Figure 17: Force acting on barge during 0^0 wave heading

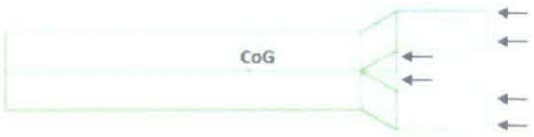

Figure 18: Force acting on barge during 180^0 wave heading

With 180^0 wave heading, the wave is attacking onto the exposed forked stern as compared to 0^0 whereby the forked section is sheltered. This means the force is exerted close to the CoG (Centre of Gravity) thus the barge exhibited a more intense response as proven by results shown above for surge, heave and pitch direction and also clearly revealed in the zoomed in plot.

Detailed calculation of RAO for varying barge draft is attached in APPENDIX F.

4.6 Modelling tests results

Modelling tests were again, only conducted for reference data with a wave heading of 180^0.

4.6.1 Wave probe data

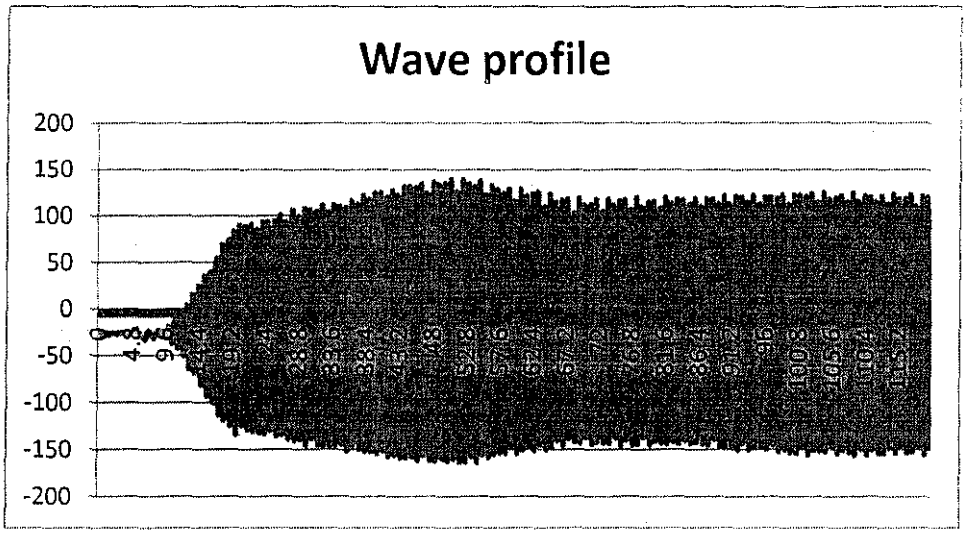

Shown above is a plot of wave height data collected automatically using wave probe. Plotting the filtered and scaled up data against time, I arrive at the wave profile with H_{max} of 164.32m. Wave amplitude is thus half of that value which is 82.16m.

4.6.2 Optical tracking system data

Surge

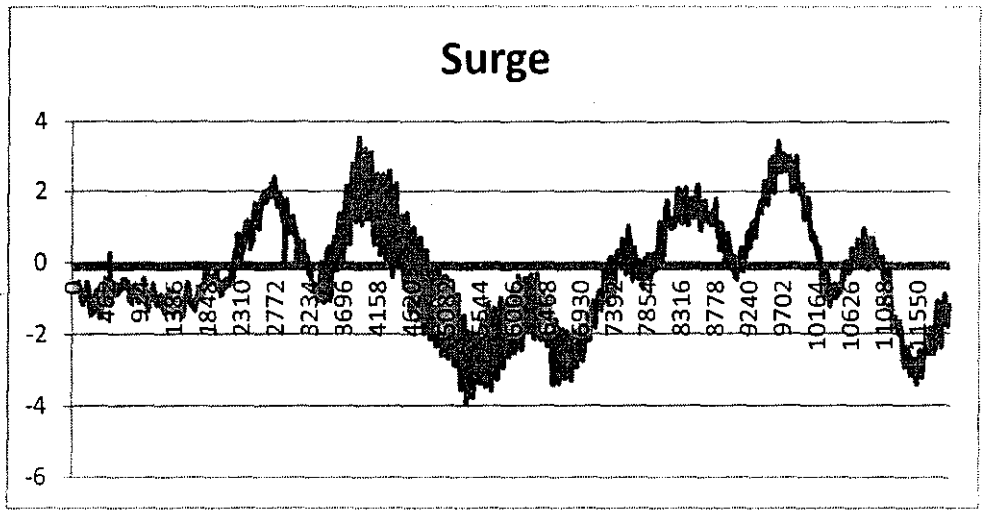

Scaled up responses in the surge direction plotted against time yield the graph shown above where:

Max surge = 3.9351m

$$RAO = \frac{H_{surge}}{H_{max}} = \frac{3.9351}{82.16} = 0.047897009$$

Pitch

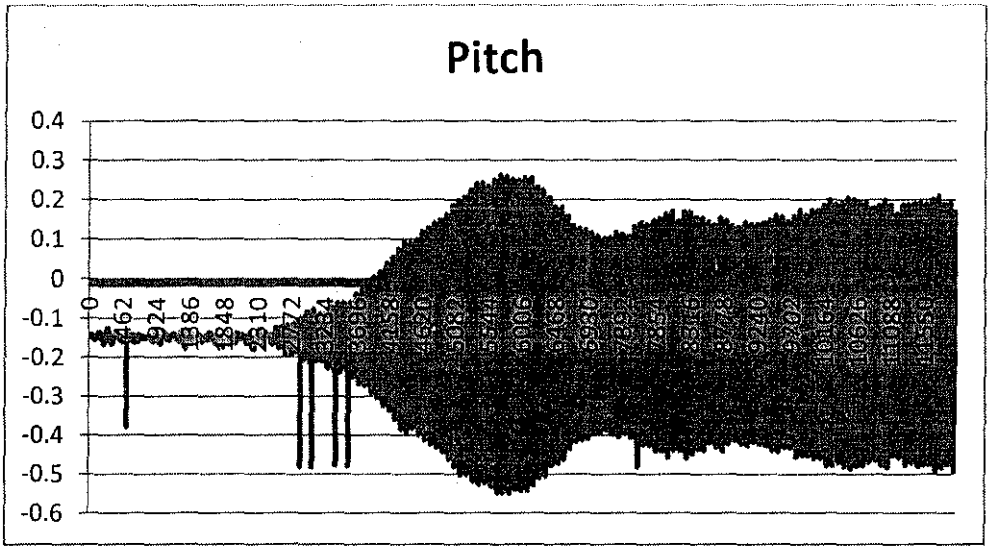

Max pitch = 0.5479812 m

$$RAO = \frac{H_{pitch}}{H_{max}} = \frac{0.5479812}{82.16} = 0.006669884$$

Heave

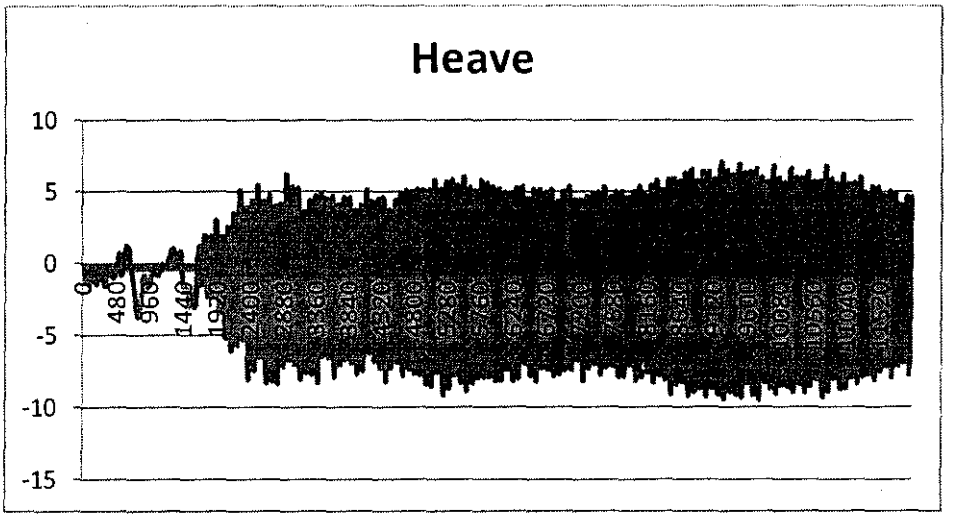

Max heave = 9.47885 m

$$RAO = \frac{H_{heave}}{H_{max}} = \frac{9.47885}{82.16} = 0.115374085$$

4.6.3 Comparison between theoretical and experimental results

Motion direction	Theoretical	Experimental	Error
Surge	0.069516577	0.047897009	31.10%
Pitch	0.010439268	0.006669884	36.11%
Heave	0.906442373	0.115374085	87.27%

For surge and pitch direction, error range of approximately 30% is acceptable due to certain assumptions made in theoretical analysis and also human or calibration errors during model testing. However, calculated error for pitch direction of 87.27% is certainly beyond the acceptable error range. Thus, further solidifying the dynamic amplification issues with motions in the heave direction as highlighted in the previous sections. To rectify such error, the Pressure Area method was used to determine whether a change in theoretical formula would generate more accurate results.

4.7 Pressure Area method

4.7.1 Heave motions for varying barge draft

Barge draft	2m	4m	6.75m
Max F_x	2.317088308	2.071943966	1.776649538
RAO	0.092452084	[redacted]	0.075283689
H surge	0.171960877	0.604490354	0.140027662

Comparing RAO of 0.324994814 for reference data (4m) with experimental results of 0.115374085, the error was reduced to 65% from 88%. Using the Pressure Area method as an alternative to Froude-Krylov calculations, I arrived at results with reduced error but the value obtained is still unsatisfactory. This in direct means that the results for heave are flawed and thus RAO effects to varying parameter in that direction are not in accordance to those observed in surge and pitch.

CHAPTER 5

CONCLUSION AND RECOMMENDATIONS

5.1 Conclusion

As a conclusion, model tests for reference data and numerical analysis to achieve parametric comparison have been completed. Generally, only barge draft and wave period bears significance on the barge motions in all concerned direction (surge, pitch, heave). But, for heave motions, in addition to draft and wave period, mooring line stiffness also has a substantial effect on barge motions in that direction. This effect that mooring line stiffness has on heave motions is far more valid as compared to motions in other direction. Thus, it can be concluded based on my study and other research done that mooring the barge onto seafloor is more conducive in restricting heave motions. However, this cannot be treated as a definite conclusion as there is no supporting proof to that statement.

Effects of water depth are minimal but the deeper the location is, the smaller the response RAO. Thus, floatover is better suited for deep sea platforms. Study into the effects of barge drafts, we can arrive at the conclusion that a heavier barge is more favoured for floatover operations as the weight of the barge itself stabilizes itself against waves, resulting in more controlled motions. However, that is not the case for motion in the heave direction, according to numerical analysis that I have completed. This is mainly due to assumptions made regarding the natural period and damping ratio of the structure. Hence, leading to a situation whereby the barge natural period is close to the wave period, creating dynamic amplifications. To rectify the problem, I attempted another alternative to the Froude-Krylov calculations- Pressure Area method. But the results have only accomplished at reducing the error from 82% to 67% which is beyond the error range of 30% exhibited by surge and pitch direction. Thus, it is safe to say that results rendered in the heave direction are flawed.

Study into the effects of wave period on the other hand only further proves what is already established about the relationship between RAO and frequency. With a shorter frequency (longer period), we can expect a higher RAO. But there is no linear correlation between RAO and frequency. RAO reduces as frequency increases but goes through minor fluctuation along the frequency scale. For wave direction however, I arrived at the conclusion that the closer the force exertion point is to the barge Centre of Gravity (CoG) the larger the response is. Therefore, the response might be at its peak during a oblique wave direction of 45^0 and 90^0. Again, this must be ascertained via modelling tests.

5.2 Recommendations

The recommendations are as following:

(a) Natural period and damping ratio in the heave direction

Decay tests weren't completed in the heave direction due to overdamping reasons. Modifications can be done to the test but that would require extensive research and would probably be cost consuming. For further studies, reference can be made to other relevant researches to assimilate the heave period and damping ratio calculated. A research on floating platform yielded such results:

	Surge	Heave	Roll	Pitch
Full draft (with risers)	11.0 % (-97.5 ~ -12.2 m)	6.5 % (10.9 ~3.2 m)	0.86 % (5 ~ 4.2 deg)	6.7 % (5 ~ 1.4 deg)
Full draft (w/o risers)	5.8 % (-96.7 ~-32.7 m)	6.1 % (10.4 ~3.3 m)	0.68 % (5 ~ 4.4 deg)	6.0 % (5 ~ 1.6 deg)

	Surge	Heave	Roll	Pitch
Full draft (with risers)	209.8 s	18.7 s	13.0 s	18.6 s
Full draft (w/o risers)	225.9 s	18.7 s	13.4 s	18.6 s

The natural period of 18.7s and heave of 6.5% could be assumed as that of the barge structure as both are floating structures. But, this does not guarantee that the accuracy of results obtained.

b) More extensive modelling tests

Due to time constraint, experiments were only conducted for reference data with one draft, one wave direction, one frequency. That was assumed to be sufficient for my final year project. But, completing parametric comparison, certain phenomena regarding the effects these parameters have on barge motions were discovered. Theoretically, these patterns were explainable however there is a lack of concrete proof. If this study was to be extended, validation should be done via more extensive modelling tests.

REFERENCES

[1] M. Luo, D. Edelson, Liyong Chen (2010). *Topsides Load Out to Barge Catamaran for Floatover Installation.* Retrieved from Technip France on 14th December 2011 from: http://www.faqs.org/patents/app/20100221070

[2] A. Kocaman and DJ Kim, J. Ray McDermott Engineering LLC, Houston, Texas; Seto Jian, J. Ray McDermott, Singapore (2008). *Floatover of Arthit PP Deck.* p 1-2. Retrieved on 14th December 2011 from http://e-book.lib.sjtu.edu.cn/otc-2008/pdfs/otc19230.pdf

[3] Ted Moon (2008). *Floatover Installations on the rise* for Society of Petroleum Engineers (SPE). Retrieved on 20th June 2011 from: http://www.kbr.com/Newsroom/Publications/articles/Floatover-Installations-on-the-Rise.pdf

[4] E. Hussain (2011). *Offshore Floatover Platform Installation* for Arabian Oil & Gas. Retrieved on 14th December 2011 from: http://www.arabianoilandgas.com/article-8632-offshore-float-over-platform-installation/

[5] A.Magee, A.Sablok, B.Koo, E.Beyko, K.Lambrakos (2010, June). *Prediction of Motions and Loads for Floatover Installation of Spar Topsides.* Proceedings of the ASME 2010 29th International Conference on Ocean, Offshore and Arctic Engineering. p. 4

[6] Ben C. Gerwick, 2007. *Construction of Marine and Offshore Structures.* 3rd Edition, CRC Press. p. 633-641.

[7] *Floating Production System* (2009, August 16-21). p.117. Retrieved from ISSC Committee V2. Retrieved on 19th June 2011 from: http://www.scribd.com/doc/54605221/35/Float-Over-of-Integrated-Deck-on-Jacket-structure

[8] Alp Kocaman. *Overcoming Floatover Challenges.* Retrieved from J. Ray McDermott Inc. Retrieved on 20th June 2011 from: http://www.pennenergy.com/index/petroleum/display/327119/articles/offshore/volume-68/issue-4/field-development/overcoming-float-over-challenges.html

[9] *Turkmenistan Block 1 Gas Development Project: Gas Full Field Development Phase 1 Design Basis* for Petronas Carigali (Turkmenistan Sdn Bhd), p.10-14, 22-23,25

[10] *Turkmenistan Block 1 Gas Development Project: MCR-A Topside Floatover Manual* for Petronas Carigali (Turkmenistan Sdn Bhd), p.4-8, 24-25

[11] H.de Groot, M.Seij (2007, May). *State of the Art in FloatOvers.* OTC 19072

[12] Martin Dixen, 2009. *MCR-A Platform Model Tests (Turkmenistan Block 1)* by DHI for Technip Geoproduction (M) Sdn Bhd. p. 6, 10-11, 16-17

[13] A. Munro-Kidd, F. Wilson (2008, May 5-8). *Caspian Challenge for Marine Installation,* OTC 19237, p. 2

[14] Chakrabati S.K., 1994. *Hydrodynamics of Offshore Structures.* WIT press. p. 402, 404, 413-418

[15] Van de Boom,H.J.J, Dekker J.N, Van Elsacker, A.W (1988). *Dynamic Aspects of Offshore Riser and Mooring Concepts.* Society of Petroleum Engineers. p.1609-1616

[16] A. B. M. Saiful Islam, Mohammed Jameel, Mohd Zamin Jumaat and S. M. Shirazi (2011). *Spar Platform at Deep Water Region in Malaysian Sea.* p.6872-6881

APPENDICES

APPENDIX A

GANTT CHART OF FYP I

WEEK NUMBER / MILESTONES	1	2	3	4	5	6	7		8	9	10	11	12	13	14
BRIEFING AND TOPIC SELECTION								SEMESTER BREAK							
PRELIMINARY RESEARCH WORK															
DATA ACQUISITION															
SUBMISSION OF EXTENDED PROPOSAL															
MODELLING TESTS (PRELIMINARY)															
PROPOSAL DEFENSE															
NUMERICAL ANALYSIS (PRELIMINARY)															
DATA ANALYSIS (PRELIMINARY)															
SUBMISSION OF INTERIM REPORT															

GANTT CHART OF FYP II

WEEK NUMBER / MILESTONES	1	2	3	4	5	6	7		8	9	10	11	12	13	14
PREPARATION OF SPREADSHEETS								SEMESTER BREAK							
NUMERICAL ANALYSIS															
PARAMETRIC COMPARISON															
SUBMISSION OF PROGRESS REPORT															
MODELLING TESTS															
ANALYSIS OF MODEL TEST RESULTS															
EXHIBITION AND PRESENTATION															
FINAL REPORT SUBMISSION															

Appendix B

Numerical analysis results for surge

	30m	50m	61.7m	70m	75m
0	1.070588411	1.075555478	1.075605967	1.075605447	1.075605382
1	1.454405294	1.427043215	1.426719473	1.426718783	1.426718697
2	0.383816883	0.351487737	0.351113506	0.351113336	0.351113315
3	-1.07058841	-1.075555478	-1.075605967	-1.075605447	-1.075605382
4	-1.45440529	-1.427043215	-1.426719473	-1.426718783	-1.426718697
5	-0.38381688	-0.351487737	-0.351113506	-0.351113336	-0.351113315
6	1.070588411	1.075555478	1.075605967	1.075605447	1.075605382
Max F_x	1.454405294	1.427043215	1.426719473	1.426718783	1.426718697
RAO	0.070865562	0.069532352	0.069516577	0.069516544	0.069516539
H_{max}	1.86	1.86	1.86	1.86	1.86
H_{surge}	0.131809946	0.129330174	0.129300834	0.129300771	0.129300763

Numerical analysis results for pitch

	30m	50m	61.7m	70m	75m
0	372.5340369	364.8263207	364.7343588	364.7363409	364.735641
1	-90.48044804	-97.99247944	-98.07871762	-98.07799625	-98.07866119
2	-463.014485	-462.8188001	-462.8130764	-462.8143371	-462.8143022
3	-372.5340369	-364.8263207	-364.7343588	-364.7363409	-364.735641
4	90.48044804	97.99247944	98.07871762	98.07799625	98.07866119
5	463.014485	462.8188001	462.8130764	462.8143371	462.8143022
6	372.5340369	364.8263207	364.7343588	364.7363409	364.735641
Max F_x	463.014485	462.8188001	462.8130764	462.8143371	462.8143022
RAO	0.010443811	0.010439398	0.010439268	0.010439297	0.010439296
H_{max}	1.86	1.86	1.86	1.86	1.86
H_{surge}	0.019425489	0.129330174	0.129300834	0.129300771	0.129300763

Numerical analysis results for heave

	30m	50m	61.7m	70m	75m
0	4.229271833	4.107162547	4.105716341	4.105725371	4.105726496
1	-1.580082928	-1.672090051	-1.67313835	-1.673142029	-1.673142488
2	-5.809354762	-5.779252598	-5.778854691	-5.7788674	-5.778868984
3	-4.229271833	-4.107162547	-4.105716341	-4.105725371	-4.105726496
4	1.580082928	1.672090051	1.67313835	1.673142029	1.673142488
5	5.809354762	5.779252598	5.778854691	5.7788674	5.778868984
6	4.229271833	4.107162547	4.105716341	4.105725371	4.105726496
Max F_x	5.809354762	5.779252598	5.778854691	5.7788674	5.778868984
RAO	0.911226462	0.906504787	0.906442373	0.906444366	0.906444615
H_{max}	1.86	1.86	1.86	1.86	1.86
H_{surge}	1.69488122	1.686098903	1.685982814	1.685986522	1.685986984

Appendix C

Numerical analysis results for surge

	2m	4m	6.75m
0	0.597692859	1.075605967	1.527340215
1	0.792799656	1.426719473	2.025914781
2	0.195106797	0.351113506	0.498574566
3	-0.59769286	-1.075605967	-1.527340215
4	-0.79279966	-1.426719473	-2.025914781
5	-0.1951068	-0.351113506	-0.498574566
6	0.597692859	1.075605967	1.527340215
Max F_x	0.792799656	1.426719473	2.025914781
RAO	0.077820233	0.069516577	0.058067779
H_{max}	1.86	1.86	1.86
H_{surge}	0.144745634	0.129300834	0.108006069

Numerical analysis results for pitch

	2m	4m	6.75m
0	203.415601	364.7343588	535.4698296
1	-53.54435936	-98.07871762	-144.6989896
2	-256.9599603	-462.8130764	-680.1688192
3	-203.415601	-364.7343588	-535.4698296
4	53.54435936	98.07871762	144.6989896
5	256.9599603	462.8130764	680.1688192
6	203.415601	364.7343588	535.4698296
Max F_x	256.9599603	462.8130764	680.1688192
RAO	0.011757858	0.010439268	0.008962492
H_{max}	1.86	1.86	1.86
H_{surge}	0.021869615	0.019417039	0.016670235

Numerical analysis results for heave

	2m	4m	6.75m
0	2.281466427	4.105716341	6.032577291
1	-0.929730321	-1.67313835	-2.458361848
2	-3.211196747	-5.778854691	-8.490939139
3	-2.281466427	-4.105716341	-6.032577291
4	0.929730321	1.67313835	2.458361848
5	3.211196747	5.778854691	8.490939139
6	2.281466427	4.105716341	6.032577291
Max F_x	3.211196747	5.778854691	8.490939139
RAO	0.128127112	0.906442373	0.359794777
H_{max}	1.86	1.86	1.86
H_{surge}	0.238316428	1.685982814	0.669218285

Appendix D

Numerical analysis results for surge

	6s	8.38s	8.9s	9.0s	9.4s
0	1.075605967	1.005812408	1.881823162	1.921034979	1.645937139
1	1.426719473	2.699556836	2.699037524	2.5664172	1.754734611
2	0.351113506	2.945455834	2.225997445	2.01094429	1.10829215
3	-1.07560597	1.611627111	0.68883615	0.514528198	-0.015160616
4	-1.42671947	-0.586560872	-1.177618048	-1.222641357	-1.132088233
5	-0.35111351	-2.470160376	-2.481120859	-2.387723432	-1.761763683
6	1.075605967	-3.028945983	-2.598542639	-2.435563177	-1.633173878
Max F_x	1.426719473	3.028945983	2.699037524	2.5664172	1.645937139
RAO	0.069516577	0.289525146	0.291436328	0.283462906	0.212529386
H_{max}	1.86	1.86	1.86	1.86	1.86
H_{surge}	0.129300834	0.538516771	0.542071571	0.527241004	0.395304657

Numerical analysis results for pitch

	6s	8.38s	8.9s	9.0s	9.4s
0	364.7343588	689.5348679	534.4834988	486.6315736	287.5465516
1	-98.07871762	394.441901	131.5146624	81.51575815	-80.82325834
2	-462.8130764	-112.2009382	-334.323762	-361.7421865	-414.4066385
3	-364.7343588	-558.667376	-640.3412447	-635.7369418	-569.6288919
4	98.07871762	-705.5053724	-640.2484462	-612.2633166	-479.68217
5	462.8130764	-473.9617338	-334.0897283	-302.304881	-183.2796523
6	364.7343588	11.78041673	131.7780533	149.1053682	192.006653
Max F_x	462.8130764	705.5053724	640.3412447	635.7369418	569.6288919
RAO	0.010439268	0.031567843	0.032462196	0.032986334	0.032359783
H_{max}	1.86	1.86	1.86	1.86	1.86
H_{surge}	0.019417039	0.058716188	0.060379685	0.061354582	0.060189196

Numerical analysis results for heave

	6s	8.38s	8.9s	9.0s	9.4s
0	4.105716341	11.5004717	7.776396734	6.777856081	2.963459843
1	-1.67313835	5.680466844	1.056201504	0.278307352	-1.720599386
2	-5.778854691	-3.186126197	-6.168902853	-6.351464481	-5.664110523
3	-4.105716341	-10.34391348	-10.44500993	-10.00931549	-7.169781527
4	1.67313835	-11.95397987	-9.727959143	-8.983696546	-5.589569748
5	5.778854691	-7.152803166	-4.360531178	-3.754506142	-1.603600277
6	4.105716341	1.484615565	3.091415684	3.231459413	3.072560725
Max F_x	5.778854691	11.95397987	10.44500993	10.00931549	7.169781527
RAO	0.906442373	0.486688274	0.388756753	0.367090914	0.249486859
H_{max}	1.86	1.86	1.86	1.86	1.86
H_{surge}	1.685982814	0.90524019	0.72308756	0.682789101	0.464045557

Appendix E

Numerical analysis results for surge

	0.131356843	0.157628212	0.18389958	0.105085475	0.078814106
0	1.075605967	1.075605967	1.075605967	1.075605967	1.075605967
1	1.426719473	1.426719473	1.426719473	1.426719473	1.426719473
2	0.351113506	0.351113506	0.351113506	0.351113506	0.351113506
3	-1.07560597	-1.075605967	-1.075605967	-1.075605967	-1.075605967
4	-1.42671947	-1.426719473	-1.426719473	-1.426719473	-1.426719473
5	-0.35111351	-0.351113506	-0.351113506	-0.351113506	-0.351113506
6	1.075605967	1.075605967	1.075605967	1.075605967	1.075605967
Max F_x	1.426719473	1.426719473	1.426719473	1.426719473	1.426719473
RAO	0.069516577	0.069599262	0.069682144	0.069434088	0.069351794
H_{max}	1.86	1.86	1.86	1.86	1.86
H_{surge}	0.129300834	0.129454628	0.129608787	0.129147404	0.128994337

Numerical analysis results for pitch

	944.487666	1133.385199	1322.282732	755.5901328	566.6925996
0	364.7343588	364.7343588	364.7343588	364.7343588	364.7343588
1	-98.07871762	-98.07871762	-98.07871762	-98.07871762	-98.07871762
2	-462.8130764	-462.8130764	-462.8130764	-462.8130764	-462.8130764
3	-364.7343588	-364.7343588	-364.7343588	-364.7343588	-364.7343588
4	98.07871762	98.07871762	98.07871762	98.07871762	98.07871762
5	462.8130764	462.8130764	462.8130764	462.8130764	462.8130764
6	364.7343588	364.7343588	364.7343588	364.7343588	364.7343588
Max F_x	462.8130764	462.8130764	462.8130764	462.8130764	462.8130764
RAO	0.010439268	0.010480707	0.010522474	0.010398156	0.010357366
H_{max}	1.86	1.86	1.86	1.86	1.86
H_{surge}	0.019417039	0.019494114	0.019571802	0.01934057	0.0192647

Numerical analysis results for heave

	48.4055381	58.08664572	67.76775334	38.72443048	29.04332286
0	4.105716341	4.105716341	4.105716341	4.105716341	4.105716341
1	-1.67313835	-1.67313835	-1.67313835	-1.67313835	-1.67313835
2	-5.778854691	-5.778854691	-5.778854691	-5.778854691	-5.778854691
3	-4.105716341	-4.105716341	-4.105716341	-4.105716341	-4.105716341
4	1.67313835	1.67313835	1.67313835	1.67313835	1.67313835
5	5.778854691	5.778854691	5.778854691	5.778854691	5.778854691
6	4.105716341	4.105716341	4.105716341	4.105716341	4.105716341
Max F_x	5.778854691	5.778854691	5.778854691	5.778854691	5.778854691
RAO	0.906442373	0.398044803	0.247987679	1.011540595	0.422870076
H_{max}	1.86	1.86	1.86	1.86	1.86
H_{surge}	1.685982814	0.740363333	0.461257082	1.881465506	0.786538341

Appendix F

Numerical analysis for surge

	180°	0°
0	1.075605967	-0.348078755
1	1.426719473	-1.400307444
2	0.351113506	-1.052228689
3	-1.07560597	0.348078755
4	-1.42671947	1.400307444
5	-0.35111351	1.052228689
6	1.075605967	-0.348078755
Max F_x	1.426719473	1.400307444
RAO	0.069516577	0.068229657
H_{max}	1.86	1.86
H_{surge}	0.129300834	0.126907162

Numerical analysis for pitch

	180°	0°
0	364.7343588	-452.0092489
1	-98.07871762	-105.494933
2	-462.8130764	346.5143159
3	-364.7343588	452.0092489
4	98.07871762	105.494933
5	462.8130764	-346.5143159
6	364.7343588	-452.0092489
Max F_x	462.8130764	452.0092489
RAO	0.010439268	0.010195576
H_{max}	1.86	1.86
H_{surge}	0.019417039	0.018963771

Numerical analysis for heave

	180°	0°
0	4.105716341	-5.663871575
1	-1.67313835	-1.626159443
2	-5.778854691	4.037712133
3	-4.105716341	5.663871575
4	1.67313835	1.626159443
5	5.778854691	-4.037712133
6	4.105716341	-5.663871575
Max F_x	5.778854691	5.663871575
RAO	0.906442373	0.888406694
H_{max}	1.86	1.86
H_{surge}	1.685982814	1.652436451